

Elsevier Editorial System(tm) for  
Translational Research  
Manuscript Draft

Manuscript Number: TR-15-328R2

Title: N-bromotaurine surrogates for loss of antiproliferative response and enhances cisplatin efficacy in cancer cells with impaired glucocorticoid receptor

Article Type: Full Length Article

Keywords: GR; glucocorticoid resistance; N-bromotaurine; skin carcinogenesis; drug re-purposing

Corresponding Author: Prof. Vassilis Zoumpourlis, PhD

Corresponding Author's Institution: National Hellenic Research Foundation

First Author: Stella Logotheti, PhD

Order of Authors: Stella Logotheti, PhD; Nikolas Khoury; Spiros A Vlahopoulos, PhD; Elena Skourti, MSc; Dimitra Papaevangeliou, PhD; Triantafyllos Liloglou, PhD; Vassilis Gorgoulis, MD, PhD; Irina Budunova, PhD; Anthony M Kyriakopoulos, MD, PhD; Vassilis Zoumpourlis, PhD

Manuscript Region of Origin: GREECE

Abstract: Glucocorticoids (GCs) are frequently used in anticancer combination regimens; however, their continuous use adds selective pressure on cancer cells to develop GC-resistance via impairment of the glucocorticoid receptor (GR), therefore creating a need for GC-alternatives. Based on the drug repurposing approach and the commonalities between inflammation and neoplasia, drugs that are either in late-stage clinical trials and/or already marketed for GC-refractory inflammatory diseases, could be evaluated as GC-substitutes in the context of cancer. Advantageously, unlike new molecular entities currently being de novo developed to restore GC-responsiveness of cancer cells, such drugs have documented safety and efficacy profile, which overall simplifies their introduction in clinical cancer trials. In this study, we estimated the potential of a well-established, multistage, cell line-based, mouse skin carcinogenesis model to be exploited as an initial screening tool for unveiling covert GC-substitutes. First, we categorized the cell lines of this model to GC-sensitive and GC-resistant, in correlation with their corresponding GR status, localization and functionality. We found that GC-resistance starts in papilloma stages, due to a dysfunctional GR, which is overexpressed, DNA binding-competent, but transactivation-incompetent in papilloma, squamous and spindle stages of the model. Then, aided by this tool, we evaluated the ability of N-bromotaurine, a naturally-occurring, small-molecule, NSAID which is under consideration for use interchangeably/in replacement to GCs in skin inflammations, to restore antiproliferative response of GC-resistant cancer cells. Unlike GCs, N-bromotaurine inhibited cell-cycle progression in GC-resistant cancer cells and efficiently synergized with cisplatin, thus indicating a potential to be exploited instead of GCs against cancer.

1  
2  
3 **N-bromotaurine surrogates for loss of antiproliferative response and enhances**  
4 **cisplatin efficacy in cancer cells with impaired glucocorticoid receptor**  
5  
6

7 Stella Logotheti<sup>1,7</sup>, Nikolas Khoury<sup>1</sup>, Spiros A. Vlahopoulos<sup>2</sup>, Elena Skourti<sup>1</sup>, Dimitra  
8 Papaevangeliou<sup>1</sup>, Triantafyllos Liloglou<sup>3</sup>, Vassilis Gorgoulis<sup>4</sup>, Irina Budunova<sup>5</sup>, Anthony M.  
9 Kyriakopoulos<sup>6</sup>, Vassilis Zoumpourlis<sup>1\*</sup>  
10

11  
12 <sup>1</sup>Biomedical Applications Unit, Institute of Biology, Medicinal Chemistry and Biotechnology,  
13 National Hellenic Research Foundation, 48 Vassileos Constantinou Avenue, 116 35 Athens,  
14 Greece.  
15

16 <sup>2</sup>Horemio Research Institute, First Department of Pediatrics, "Aghia Sophia" Children's  
17 Hospital, National and Kapodistrian University of Athens, Athens, Greece.  
18

19 <sup>3</sup>University of Liverpool, Department of Molecular and Clinical Cancer Medicine, 200 London  
20 Road, Liverpool L3 9TA, UK  
21

22 <sup>4</sup>Laboratory of Histology-Embryology, Molecular Carcinogenesis Group, Medical School,  
23 National and Kapodistrian University of Athens, Athens, Greece.  
24

25 <sup>5</sup>Department of Dermatology, Northwestern University, Chicago, IL, USA.

26 <sup>6</sup>Nasco AD, Biotechnology Laboratory, 11th Sachtouri str., Piraeus, Greece.

27 <sup>7</sup>Department of Biotechnology, Agricultural University of Athens, Athens, Greece  
28  
29

30  
31 \* Corresponding author

32 Tel: 30-10-7273730

33 Fax: 30-10-7273677

34 e-mail: vzub@eie.gr  
35  
36  
37  
38

39 Running title : Repurposing BrTaur in GC-resistant cancers  
40

41  
42 Keywords: GR; glucocorticoid resistance; N-bromotaurine; skin carcinogenesis; drug re-  
43 purposing  
44

45 Abbreviations: GC: glucocorticoid; GR: glucocorticoid receptor; GRE: glucocorticoid receptor  
46 element; NSAID: non-steroid anti-inflammatory drug; BrTaur: N-bromotaurine; CITaur: N-  
47 chlorotaurine; EMSA: electrophoretic mobility shift assay; FACS: fluorescence-activated cell  
48 sorting; qRT-PCR: quantitative Real-Time-Polymerase Chain Reaction.  
49  
50  
51  
52  
53  
54  
55  
56  
57  
58  
59  
60  
61  
62  
63  
64  
65

1  
2  
3 **ABSTRACT**

4 Glucocorticoids (GCs) are frequently used in anticancer combination regimens; however,  
5 their continuous use adds selective pressure on cancer cells to develop GC-resistance via  
6 impairment of the glucocorticoid receptor (GR), therefore creating a need for GC-alternatives.  
7 Based on the drug repurposing approach and the commonalities between inflammation and  
8 neoplasia, drugs that are either in late-stage clinical trials and/or already marketed for GC-  
9 refractory inflammatory diseases, could be evaluated as GC-substitutes in the context of  
10 cancer. Advantageously, unlike new molecular entities currently being *de novo* developed to  
11 restore GC-responsiveness of cancer cells, such drugs have documented safety and efficacy  
12 profile, which overall simplifies their introduction in clinical cancer trials. In this study, we  
13 estimated the potential of a well-established, multistage, cell line-based, mouse skin  
14 carcinogenesis model to be exploited as an initial screening tool for unveiling covert GC-  
15 substitutes. First, we categorized the cell lines of this model to GC-sensitive and GC-  
16 resistant, in correlation with their corresponding GR status, localization and functionality. We  
17 found that GC-resistance starts in papilloma stages, due to a dysfunctional GR, which is  
18 overexpressed, DNA binding-competent, but transactivation-incompetent in papilloma,  
19 squamous and spindle stages of the model. Then, aided by this tool, we evaluated the ability  
20 of N-bromotaurine, a naturally-occurring, small-molecule, NSAID which is under consideration  
21 for use interchangeably/in replacement to GCs in skin inflammations, to restore  
22 antiproliferative response of GC-resistant cancer cells. Unlike GCs, N-bromotaurine inhibited  
23 cell-cycle progression in GC-resistant cancer cells and efficiently synergized with cisplatin,  
24 thus indicating a potential to be exploited instead of GCs against cancer.  
25  
26  
27  
28  
29  
30  
31  
32  
33  
34  
35  
36  
37  
38  
39  
40  
41  
42  
43  
44  
45  
46  
47  
48  
49  
50  
51  
52  
53  
54  
55  
56  
57  
58  
59  
60  
61  
62  
63  
64  
65

## INTRODUCTION

Glucocorticoids (GCs) are steroid hormones which inhibit tumor cell proliferation, mitigate chemotherapy side effects and enhance efficiency of anticancer agents<sup>1,2</sup>. They are frequently included in combination anticancer therapies, either as palliative agents against chemotherapy-induced-nausea-and-vomiting or as antiproliferative agents. Their effects are mediated by the glucocorticoid receptor (GR). GC binds to GR which, following dissociation from a cytoplasmic chaperone/co-chaperone complex, translocates to the nucleus, homodimerizes and regulates gene expression. GR transactivates or transrepresses genes by direct binding to GREs (glucocorticoid responsive elements), by tethering itself to other transcription factors apart from DNA binding, or in a composite manner by both direct GRE binding and interactions with transcription factors bound to neighboring sites (reviewed by Ramamoorthy et al<sup>2</sup>). Thus, a functional GR elicits tumor-suppressive events in a pleiotropic manner, through a plethora of mechanisms and crucial pathways.<sup>3-5</sup>

Theoretically, the clinical benefits demonstrated by the long-term experience on GCs, combined with the tumor-suppressive nature of GR, offer a strong alibi for their routine use in cancer therapeutics (e.g. prostate cancer, breast cancer, leukemia), as evidenced by the increasing number of GC-containing combination regimens, both established and investigational. Nevertheless, GC cotreatment often induces resistance towards cancer therapy<sup>1,6</sup> thus raising concerns regarding the tendency of GC-sensitive cancer cells to develop resistance upon frequent GC use. Mechanistically, this tendency is attributed to the pleiotropic nature of GR *per se*. GR's pleiotropy becomes a double-edged sword, since cancer cells have, at their disposal, as many potentials to overcome GR's antiproliferative barrier and achieve GC-resistance, as is the plethora of underlying GR-mediated antiproliferative pathways they can defuse one way or another. For neutralizing GR antiproliferative effects, cancer cells exploit several strategies, which in several cases simultaneously co-exist in a cancer cell (e.g. reduced GR expression, reduced DNA binding ability, GR mutations and polymorphisms, co-expression of dominant negative GR isoforms, impairment of transrepression mode et.c.).<sup>2,7,8</sup> GC-unresponsiveness by GR impairment may start as early as the benign stages, highlighting that inactivation of GC/GR axis is a selective advantage in order for a cancer cell to surpass the antiproliferative break and continue its tumorigenic march towards aggressive stages.<sup>9</sup>

This overall necessitates alternatives restoring and/or surrogating for GCs' antiproliferative effects.<sup>2,10</sup> To this end, innovative synthetic molecules are being developed by academia, aiming to re-activate GR-mediated antiproliferative pathways and restore GC-responsiveness of cancer cells<sup>10</sup>. If they successfully pass clinical trials, they will eventually find their way to the bedside. But this established bench-to-bedside pipeline is not an one-way street. The recently framed concept of drug repurposing suggests evaluating suitability of

1  
2  
3 known drugs for use in new indications<sup>11</sup>. Implementing this concept in the issue of GC-  
4 resistance, we postulate that drugs which are already in late stages of clinical trials or  
5 approved for indications other than cancer may be latent GC-substitutes, able to imitate  
6 aspects of the GC therapeutic profile. These hypothetical latent GC-substitutes might be  
7 competent to either restore the antiproliferative phenotypes in GC-resistant cells; or to be  
8 used interchangeably to GCs, in order to reduce the selective pressure exerted by continuous  
9 use of GCs on GC-sensitive cells, thus preventing/delaying their clonal expansion to GR-  
10 impaired and, hence, GC-resistant cells. A clinical advantage of the proposed approach is  
11 that these candidate substances are actually closer to the bedside than they are to the bench,  
12 since they have a more characterized efficacy and safety profile, in terms of their  
13 documentation for other therapeutic indications. This is translated to both faster filing and  
14 regulatory approval procedures and to reduced financial costs to develop these substances  
15 as anticancer agents, compared to starting the anticancer drug research-and-development  
16 workflow from scratch, i.e. by developing New Molecular Entities (NMEs, defined by FDA as  
17 experimental substances without precedent among regulated and approved drug products).<sup>11</sup>

18  
19 Except for anticancer agents, GCs are also common anti-inflammatory agents. In fact,  
20 their use against inflammations historically preceded their use against neoplasias. GC-  
21 resistance is a frequent problem in inflammations as well, and drugs are being developed in  
22 replacement of GC-containing anti-inflammatory regimens.<sup>12</sup> Emerging GC-substitutes that  
23 are currently in the investigational clinical setting for inflammation management include, but  
24 are not limited to, the NSAID (Non-Steroid Anti-Inflammatory Drug) taurine haloamine  
25 derivatives, mainly N-bromotaurine (BrTaur) and N-chlorotaurine (ClTaur). These are  
26 generated by eosinophils and neutrophils at a site of inflammation and exert potent anti-  
27 inflammatory properties. Other common features shared with GCs is their naturally-occurring  
28 and small-molecule nature and their immunomodulatory and antimicrobial properties<sup>13</sup>.  
29 Another common characteristic is the potential to ameliorate chemotherapy-induced nausea  
30 and vomiting, since their maternal substance, i.e. the non-essential aminoacid taurine, which  
31 is orally administered as a pro-drug in order to be converted to the haloamine derivative at  
32 the site of inflammation, was recently proven clinically capable of such an effect in leukemic  
33 patients.<sup>14</sup> Advantageously, taurine haloamines have shown good efficacy, tolerance and  
34 insignificant toxic effects upon topical use on clinical patients who are refractory to  
35 conventional GC-based anti-inflammatory therapies<sup>13,15,16</sup>. Based on the association between  
36 chronic inflammatory diseases and neoplasias,<sup>17,18</sup> we postulated that a drug which exerts  
37 overlapping features and common therapeutic indications with GCs and is able to surrogate  
38 for GCs in GC-resistant inflammations may be able to surrogate for the GCs' antiproliferative  
39 function in GC-resistant cancer cells as well.

40  
41  
42  
43  
44  
45  
46  
47  
48  
49  
50  
51  
52  
53  
54  
55  
56  
57  
58  
59  
60  
61  
62  
63  
64  
65

1  
2  
3 As a springboard for testing this hypothesis, we took advantage of our long-term  
4 experience on a well-established mouse model of skin carcinogenesis.<sup>19</sup> This comprises of a  
5 series of cell lines which represent different stages of mouse skin tumor progression and are  
6 categorized on the basis of increasing aggressiveness to immortalized keratinocytes (C5N),  
7 benign papillomas (P6), malignant squamous carcinomas (B9), and highly invasive spindle  
8 cells (A5, CarB).<sup>19</sup> The B9:A5 pair represents the clonal expansion from squamous to spindle  
9 stages. The model has been developed in Dr. A. Balmain's lab and has been thoroughly  
10 reviewed<sup>18</sup> and described previously.<sup>20</sup> Briefly, in order to obtain these cell lines, each of  
11 which represent the initiation, promotion or progression stages of skin carcinogenesis, a  
12 chemical carcinogenesis protocol on mice was applied. The normal epidermis of mice or  
13 normal epithelial mouse cells were treated with a single dose of the polycyclic aromatic  
14 hydrocarbon 7,12 dimethylbenz[a]anthracene (DMBA), followed by weekly applications of the  
15 phorbol ester 12-O-tetradecanoylphorbol-13-acetate (TPA). This led to the development of  
16 numerous benign papillomas, some of which progressed to malignant squamous cell  
17 carcinomas several weeks after the first exposure to carcinogens and cell lines were  
18 produced from these tumors. Overall, this model poses the following advantages: a) it is  
19 multistage, meaning that it simulates the step-wise manner by which a tumor initiates,  
20 promotes and progresses, b) it is coherent, since cell lines have been derived in a consistent  
21 manner following a meticulous chemical carcinogenesis protocol, c) although skin-tissue  
22 based, it further applies to almost all epithelial cancers.<sup>21</sup> Furthermore, the fact that the model  
23 is skin tissue-based facilitates our analysis, because skin cancer is a traditional field where  
24 the mechanisms of GR function in correlation to GC-responsiveness have been adequately  
25 studied.<sup>4,5,9</sup> Therefore, although our model has never been characterized before in terms of  
26 GC-responsiveness, it stood a good chance to faithfully mirror or even complement previous  
27 robust findings.

28 First, we characterized our system in terms of antiproliferative response to GCs. Then, we  
29 correlated this responsiveness to the underlying GR expression status, localization and  
30 functionality. Finally, we checked the ability of BrTaur to bypass GC-resistance of cancer cells  
31 either alone or in combination with cisplatin.

## 32 **MATERIALS AND METHODS**

### 33 ***Cells and culture conditions***

34 Mouse cell lines of the mouse skin carcinogenesis model have been produced and obtained  
35 by Dr. Allan Balmain. All human cell lines used were obtained by American Type Culture  
36 Collection (ATCC). Cells were cultured as previously described.<sup>22</sup> The preparation<sup>23</sup> and use  
37  
38  
39  
40  
41  
42  
43  
44  
45  
46  
47  
48  
49  
50  
51  
52  
53  
54  
55  
56  
57  
58  
59  
60  
61  
62  
63  
64  
65

1  
2  
3 of BrTaur is covered by licensing agreement. The in-house formulation was donated by  
4 NASCO AD Biotechnology Laboratory for preclinical research purposes.  
5  
6

### 7 ***Proliferation assays***

8 Collectively, 2250 cells per well were seeded in 96-well plates. After cells were attached, the  
9 first measurement was taken. This time point is called 0 hours. At this point, 24h after  
10 seeding, dexamethasone (10<sup>-9</sup> – 10<sup>-6</sup>M, from a stock of 10<sup>-3</sup>M dexamethasone diluted in  
11 ethanol), BrTaur (25µM-250µM from a stock of 4mM BrTaur) or taurine (5-50mM from a  
12 stock of 200mM taurine diluted in water) was added and measurements were taken after 24,  
13 48 and 72h. For co-treatment experiments, cells were treated with either 10<sup>-7</sup>M  
14 dexamethasone or BrTaur (125, 250 or 500µM) 24-hours prior, con-currently with or 24-hours  
15 post cisplatin treatment. Untreated cells were used as controls. Following treatments, cells  
16 were fixed with 100% methanol and, then, crystal violet solution was added to each well. After  
17 a 10-minute incubation in room temperature, each well was washed 3 times with 200µL  
18 water, and plates were incubated on a shaker for 45min. Optical Density (OD) was measured  
19 at 595nm using a Tecan reader. The data was transferred to Microsoft Excel and analyzed.  
20 Background absorbance was corrected using triplicate sets of wells containing medium only  
21 (no cells) and crystal violet reagent as per experimental well. Three independent experiments  
22 were performed and each one of them included a triplicate value set.  
23  
24  
25  
26  
27  
28  
29  
30

### 31 ***RNA extraction, cDNA synthesis and qRT-PCR analysis***

32 mRNA extraction, cDNA synthesis and quantitative real-time PCR was conducted as  
33 previously described.<sup>24</sup> Primers used appear in Table I.  
34  
35

### 36 ***Preparation of cell lysates and Western blot analysis***

37 Total, cytoplasmic and nuclear cell lysates were prepared as previously described.<sup>25</sup> The  
38 primary antibody was an in-house anti-GR rabbit polyclonal antibody, clone 2F8, against  
39 aminoacids 305-427 of the N-terminal domain (kindly provided by Dr. M.N. Alexis), in a 1:500  
40 dilution. Primary anti-beta-actin antibody in a 1:1000 dilution was used as a loading control.  
41 The secondary antibody was a mouse anti-rabbit antibody (Santa Cruz Biotechnology, Santa  
42 Cruz, CA) in a 1:1000 dilution.  
43  
44  
45  
46

### 47 ***Two-stage chemical carcinogenesis protocol***

48 Tumors induced on mouse skin following a chemical carcinogenesis protocol were fixed and  
49 paraffin-embedded. Slides carrying formalin-fixed paraffin-embedded (FFPE) mouse skin  
50 papilloma and squamous and spindle tumors were prepared as previously described.<sup>22</sup> In  
51  
52  
53  
54  
55  
56  
57  
58  
59  
60  
61  
62  
63  
64  
65

1  
2  
3 vivo experiments were performed in the in-house authorized animal house. Experiments  
4 complied with the Protocol on the Protection and Welfare of Animals, as obliged by the rules  
5 of the National Hellenic Research Foundation, the regulations of the National Bioethics  
6 Committee and the article 3 of the presidential decree 160/1991 (in line with 86/609/EEC  
7 directive) regarding the welfare of experimental animals.  
8  
9

### 10 ***Immunohistochemical and immunocytochemical staining***

11 Immunohistochemical staining on FFPE sections was performed as described earlier.<sup>26</sup> The  
12 sections were stained with anti-GR, clone 2F8, in a 1:10 dilution. For the  
13 immunocytochemistry staining with anti-GR antibody 2F8, we followed the same procedure,  
14 incubation periods and reagents, by omitting the deparaffinization step.  
15  
16  
17

### 18 ***Immunofluorescence staining***

19 Cells were grown and fixed on coverslips and where subjected to immunofluorescence  
20 staining as previously described.<sup>27</sup> The slides were incubated with primary antibody anti-GR,  
21 clone M-20 (Santa Cruz Biotechnology, Santa Cruz, CA) in a 1:50 dilution. The secondary  
22 antibody was anti-rabbit FITC-conjugated (Jackson Laboratory, Bar Harbor, Maine, USA)  
23 diluted in 1:100.  
24  
25  
26  
27

### 28 ***Electrophoretic Mobility Shift assay***

29 Annealed oligonucleotides for the *human metallothionin IIA* Glucocorticoid Responsive  
30 Element (5'-TGGTACACTGTGTCCTGAATTCA-3' and 5'-  
31 TGAATTCAGGACACAGTGTACCA-3') were end-labeled with  $\gamma^{32}\text{P}$ -ATP using T4-  
32 polynucleotide kinase and the reaction products were purified on a 8% polyacrylamide gel.  
33 DNA binding reactions were performed as previously described.<sup>28</sup> For the supershift control  
34 experiment, the primary polyclonal antibody anti-GR 10-10 (kindly provided by Dr. M. Alexis)  
35 was used.  
36  
37  
38  
39  
40

### 41 ***Plasmids, transfections and luciferase reporter assay***

42 A luciferase plasmid carrying GRE sequences (17m-GRE-G-Luc), as well as a control vector  
43 carrying no GRE binding site (tata-pG13Luc) described previously<sup>29</sup> were used for  
44 transfections. Where indicated, cells were incubated with dexamethasone and transfected  
45 with by the calcium phosphate method, as described previously<sup>7</sup>. The luciferase activity was  
46 measured using a luminometer and was normalized for transfection efficiency with the  $\beta$ -  
47 galactosidase activity.  
48  
49  
50  
51

### 52 ***FACS analysis***

53  
54  
55  
56  
57  
58  
59  
60  
61  
62  
63  
64  
65



1  
2  
3 Cells were harvested, trypsinized and centrifuged at 1,000rpm for 5min, at room temperature.  
4 The pellet was resuspended in 500µL PBS, fixed with 80% ethanol, vortexed, and stained  
5 with propidium iodide (50µg/mL), in the presence of 5mmol/L MgCl<sub>2</sub> and 10µg/mL RNase A in  
6 10mmol/L Tris-HCl (pH 7.5). DNA content was analyzed on a FACSCalibur (Becton  
7 Dickinson) using the Modfit software.  
8  
9

### 10 **Statistical analysis**

11 Data are expressed as mean±SD. Each experiment was performed in triplicates. Then, the  
12 triplicate set values of three independent experiments were analyzed. For statistical analyses  
13 of proliferation assays resultsexperiments, -ANOVA utilising Dunetts' T3 post-hoc analysis the  
14 student's t-test was applied. QPCR results were evaluated using Mann-Whitney's test.  
15 Luciferase assays were analyzed using independent student's t-tests. P values of less than  
16 0.05 were considered significant.  
17  
18  
19  
20  
21  
22

Formatted: Font: (Default) Arial, 11 p

## 23 **RESULTS**

### 24 ***The antiproliferative effect of GCs is lost in the promotion and progression stages of*** 25 ***mouse skin carcinogenesis***

26 Our first priority was to explore the GC antiproliferative effect on the cell lines of our system.  
27 GC effect ranges from proliferative in very low concentrations, to cytostatic/antiproliferative in  
28 more physiological concentrations and cytotoxic/apoptotic in higher concentrations.<sup>30</sup> To  
29 monitor GC effect on our system, we treated cells with a range of dexamethasone  
30 concentrations previously demonstrated to show antiproliferative effects on mouse  
31 keratinocytes (10<sup>-9</sup>M - 10<sup>-6</sup>M),<sup>9</sup> and subjected them to proliferation assay. Consistent with  
32 previous similar findings,<sup>9</sup> only the immortalized C5N cells were growth-inhibited by  
33 dexamethasone, in a concentration-dependent manner. P6, B9, A5 and CarB cells continued  
34 to proliferate despite dexamethasone presence (Fig. 1a). Dexamethasone induced no effect  
35 in P6, B9, A5 and CarB cells, neither proliferative nor antiproliferative. On the other hand,  
36 each tested dexamethasone concentration reduced proliferation rate of the GC-responsive  
37 C5N cells in a time-dependent manner (Fig. 1b). ANOVA utilising Dunetts' T3 post-hoc  
38 analysis demonstrated that C5N cells showed significant sensitivity to dexamethasone. In  
39 particular, at 72 hours, significant loss of survival was observed at 10<sup>-8</sup>, 10<sup>-7</sup>, and 10<sup>-6</sup>  
40 concentrations (p=0.014, p=0.002, p<0.001 respectively). On the contrary, no significant  
41 difference observed between the untreated and treated P6 cells at any dexamethasone  
42 concentration (Fig. 1b). Therefore, the cells of our system were categorized to GC-sensitive  
43 (C5N; susceptible to growth inhibition by GCs) and to GC-resistant (P6, B9, A5 and CarB; no  
44 response to GCs, neither proliferative nor antiproliferative).  
45  
46  
47  
48  
49  
50  
51  
52  
53  
54  
55  
56  
57  
58  
59  
60  
61  
62  
63  
64  
65

Formatted: Superscript

Formatted: Superscript

Formatted: Superscript

1  
2  
3  
4 ***GR expression and localization status in the multistage mouse skin carcinogenesis***  
5 ***model***  
6

7 Then, we monitored GR expression and localization in each cell line of our model. First,  
8 western blot revealed an elevation of total GR levels towards more aggressive cancer stages.  
9 Nuclear GR levels gradually increase, showing an abrupt increase during B9-to-A5 transition,  
10 whereas there is a reduction of cytoplasmic GR protein levels from B9 to A5 cells,  
11 documenting a switch of the cytoplasmic-to-nuclear ratio upon B9/A5 transition, which is  
12 independent from GC presence (Fig. 2b). This tendency of GR to translocate to the nucleus  
13 during squamous-to-spindle transition was further confirmed by immunocytochemistry, which  
14 revealed cytoplasmic GR localization in C5N, P6 and B9 cells, and mixed cytoplasmic-  
15 nuclear localization in A5 and CarB cells (Fig. 2c). The GR nucleocytoplasmic translocation at  
16 the squamous-to-spindle threshold was additionally confirmed by immunofluorescence in B9  
17 and A5 cells, which revealed a clear cytoplasmic signal in B9 cells, but an intense nuclear  
18 staining in A5 cells (Fig. 2d). To the best of our knowledge, this mixed cytoplasmic and  
19 nuclear GR localization in aggressive stages has never been reported before. To exclude the  
20 possibility that this observation is a cell-line artefact, we confirmed it immunohistochemically  
21 *in vivo*, on sections from skin tumors induced in mice following a chemical carcinogenesis  
22 protocol. Indeed, on tumors of the same animal, papilloma stage presents mainly cytoplasmic  
23 GR localization whereas in the corresponding squamous stage GR localization is more  
24 intense and gets even more intense in the spindle stage-tumors (Fig. 2e).  
25  
26  
27  
28  
29  
30  
31  
32

33 ***GR is GRE-binding competent but transactivation-incompetent in the GC-resistant***  
34 ***cells of the mouse skin carcinogenesis model***  
35

36 Then, we tested whether GC-unresponsiveness of P6, B9, A5 and CarB cells is associated  
37 with reduced DNA binding of GR to GRE-containing targets. EMSAs were performed using  
38 nuclear cell extracts of C5N, P6, B9, A5 and CarB incubated with a <sup>32</sup>P-labelled double  
39 stranded oligonucleotide that contains a GRE binding site from the human metallothionin II  
40 promoter (hMTII-GRE). The binding of GR to GREs remains ligand-dependent only in the  
41 GC-sensitive C5N cell line (Fig. 3a), in contrast to the GC-resistant P6, B9, A5 and CarB  
42 cells, in which GR has acquired the ability to bind to GREs in the absence of dexamethasone  
43 (Fig. 3b). Additionally, the pattern of GR DNA binding along the five cell lines is consistent  
44 with their nuclear GR expression profile. This evidence indicates that the ability of GR to bind  
45 to GRE-containing targets through its DNA binding domain remains intact and proportional to  
46 the nuclear GR levels (Fig. 3b). Therefore, we plausibly hypothesized that although GR binds  
47 to target GREs in a ligand-independent manner in the P6, B9, A5 and CarB cells, it might be  
48 incapable of transactivating its targets, thus providing a reason for their GC-resistance. To  
49  
50  
51  
52  
53  
54  
55  
56  
57  
58  
59  
60  
61  
62  
63  
64  
65

1  
2  
3 this end, we then tested whether unresponsiveness of GC-resistant cells to GCs might be  
4 associated with inability of GRE-bound GR to transactivate crucial antiproliferative targets.  
5 We used luciferase assays to monitor the ability of endogenous GR to activate the  
6 glucocorticoid-responsive enhancer of  $\beta$ -globin in the presence of dexamethasone in all  
7 mouse cell lines (Fig. 3c). Significant luciferase activity was observed only in the GC-sensitive  
8 C5N cells upon GC treatment. In parallel, using Q-PCR, we estimated the endogenous  
9 expression of the characteristic GC-responsive antiproliferative direct GR targets p57<sup>KIP2</sup><sup>31</sup>  
10 and GILZ (Glucocorticoid-induced leucine zipper)<sup>32</sup> in dexamethasone-treated versus  
11 dexamethasone-untreated cells. In agreement with the luciferase assay findings, both targets  
12 were significantly induced (~~t-test, p<0.05~~) in the GC-responsive C5N cells upon  
13 dexamethasone treatment, whereas the corresponding levels were not upregulated after  
14 addition of dexamethasone in all GC-resistant cells (Fig. 3d and 3e). However, sequencing  
15 analysis revealed that this impairment is not attributed to direct mutations in the domains of  
16 the GR gene that are responsible for the GR transactivation function (Supplementary Material  
17 1).

#### 25 ***N-bromotaurine induces antiproliferative effects in GC-resistant cancer cell lines***

26 Then, we checked whether BrTaur restores antiproliferative response in our model system.  
27 To this end, we treated cells with 25 $\mu$ M, 75 $\mu$ M, 125 $\mu$ M and 250 $\mu$ M BrTaur and subjected  
28 them to proliferation assays. This range is consistent with the therapeutic concentrations  
29 currently used, in the investigational clinical setting against inflammatory conditions and  
30 microbial infections.<sup>13,15</sup> BrTaur exerted a potent, dose-dependent antiproliferative effect in  
31 the GC-sensitive C5N and the GC-resistant P6, B9, A5 and CarB cells, which is evidenced  
32 from 125 $\mu$ M (Fig. 4a). The maternal substance taurine, from which BrTaur is produced upon  
33 reduction with HOBr, has been previously reported to exert anticancer properties<sup>33,34</sup>.  
34 Therefore, we treated cell lines with the concentration range of unbrominated taurine that  
35 corresponded to the tested concentration range of its brominated derivatives<sup>23</sup>. Taurine  
36 treatment did not affect mouse skin cancer cell proliferation in a significant, potent and  
37 consistent manner (Fig. 4b), implying that bromination of the taurine is the crucial factor for  
38 the consistent antiproliferative effect on cells. ANOVA utilising Dunetts' T3 post-hoc analysis  
39 demonstrated that P6 cells showed significant sensitivity at concentrations over 75 $\mu$ M  
40 bromotaurine. A5, B9 and CarB cell lines demonstrated sensitivity at concentrations over  
41 125 $\mu$ M bromotaurine. The GC-responsive, C5N cells are the least sensitive to bromotaurine.  
42 The BrTaur antiproliferative effect was reproduced in GC-resistant human cancer cells of  
43 epithelial origin, i.e. the prostate cancer cell line PC3 (Fig. 4c) and the breast cancer cell line  
44 MDA-MB-231 (Fig. 4d)<sup>35,36</sup> in the tested concentration range.  
45  
46  
47  
48  
49  
50  
51  
52  
53  
54  
55  
56  
57  
58  
59  
60  
61  
62  
63  
64  
65

Formatted: Font: (Default) Arial, 11 p

Formatted: Font: (Default) Arial, 11 p

Formatted: Font: (Default) Arial, 11 p

Formatted: Font: (Default) Arial, 11 p

Formatted: Font: (Default) Arial, 11 p

Formatted: Font: (Default) Arial, 11 p

1  
2  
3 ***N-bromotaurine inhibits cell cycle progression in GC-resistant cells***

4 Unlike dexamethasone (Fig. 5a), BrTaur induced antiproliferative effects on the GC-resistant,  
5 aggressive CarB cells in a concentration- and time- dependent manner (Fig. 5b). GCs inhibit  
6 cancer cell growth, at least in part, by blocking cell cycle at the G0/G1 phase. This ability of  
7 GCs to induce G1-arrest is often compromised in GC-resistant cancer cells.<sup>30</sup> In this context,  
8 we examined whether BrTaur bypasses lack of antiproliferative response in the GC-resistant  
9 cells by restoring G1-arrest. Using FACS analysis, we estimated the effect of three different  
10 BrTaur concentrations (125µM, 250µM and 500µM) on the G0/G1, S and G2/M phases, using  
11 the most aggressive GC-resistant cell line of our model system, i.e. CarB. Dexamethasone  
12 was used as the comparator substance and untreated cells were used as negative control.  
13 Dexamethasone was unable to induce G1-arrest, thus having an effect on cell cycle  
14 progression identical to the one observed for the GC-untreated cells. On the contrary, BrTaur  
15 in the concentrations of 125µM and 250µM enhanced the percentage of cells in G1 phase,  
16 thus simulating the effect of GCs on cell cycle. Interestingly, in the high, yet clinically  
17 physiological, concentration of 500µM, BrTaur potently affected both G1 and G2 phases,  
18 demonstrating a broader ability to target cell cycle. Its effect on the S phase is moderate and  
19 seems to be dose-dependent (Fig. 5c). The experiment was performed in triplicates and  
20 presented a p value <0.05 (t-test).  
21  
22  
23  
24  
25  
26  
27  
28

29 ***Cisplatin efficacy on GC-resistant cells is potentiated by N-bromotaurine: the earlier the***  
30 ***initiation of N-bromotaurine co-administration, the more enhanced the synergistic***  
31 ***effect***

32  
33 In clinical cancer therapeutics, GCs are routinely co-administered with cisplatin, either as  
34 adjuvant agents or to mitigate cisplatin adverse events. Therefore, for a substance to  
35 clinically qualify as a GC-substitute in the context of cancer, it should be able to enhance  
36 cisplatin's effects on tumor growth. To test if this applies for N-bromotaurine, we treated the  
37 GC-resistant aggressive spindle CarB cells of the mouse carcinogenesis model with a  
38 combination regimen of cisplatin plus N-bromotaurine. Three treatment schemes were used:  
39 a) pre-treatment, i.e. BrTaur 0-48h, followed by cisplatin 24-48h; b) concurrent treatment, i.e.  
40 BrTaur plus cisplatin, 0-48h; c) post-treatment, i.e. cisplatin 0-24h, followed by BrTaur 24-  
41 48h. Since the qualitative effect of BrTaur on cell cycle progression is dose-dependent for the  
42 higher 250µM (affects G1) and 500µM (affects both G1 and G2) concentrations (Fig. 5c), we  
43 tested both concentrations in the BrTaur-containing combination regimens. Each scheme was  
44 compared versus its corresponding comparator combination regimen of cisplatin plus 10<sup>-7</sup>M  
45 dexamethasone. Strikingly, both BrTaur concentrations in all-three schemes synergized  
46 efficiently with 2.9µg/mL cisplatin (a value corresponding to the cisplatin concentration  
47 efficient to kill 27% of CarB cells; CarB IC50:3.7µg/mL) (Supplementary Material 2),  
48  
49  
50  
51  
52  
53  
54  
55  
56  
57  
58  
59  
60  
61  
62  
63  
64  
65

1  
2  
3 demonstrating significant superiority versus the corresponding comparator cisplatin plus  
4 dexamethasone regimens (Fig. 5d-f). ANOVA applying Dunnet's T3 post-hoc test showed  
5 that both BrTaur concentrations were efficient in all-three schemes ( $p \leq 0.001$ ). The most  
6 potent synergistic effect was observed for the pre-treatment scheme, where both doses of  
7 250 $\mu$ M and 500 $\mu$ M achieved similar efficacy. The synergistic effect was dose-dependent in  
8 concurrent treatment and post-treatment protocols. On the contrary, dexamethasone addition  
9 did not result to significant increase of the anti-proliferative effect of the regimen, either  
10 before, concurrently or following cisplatin treatment. Overall, the earlier the BrTaur co-  
11 administration started, the better its synergistic effect with cisplatin on CarB cell growth  
12 inhibition. Among the three treatment schemes, the inhibitory effect of cisplatin on cell growth  
13 was less potent in the post-treatment protocol; however higher doses of BrTaur were able to  
14 compensate for the delay of initiation of BrTaur co-administration (Fig 5f, fourth column).  
15  
16  
17  
18  
19  
20

## 21 DISCUSSION

22 Analogous to the microbes that develop a plethora of strategies to eventually become  
23 resistant to antibiotics, cancer cells invent several strategies to impair GR and overcome GC-  
24 sensitivity.<sup>2</sup> In several cases, a singleton cause of impairment cannot be identified, because  
25 GC-resistance is rather multifactorial and attributed to orchestrated inactivation of several  
26 GR-controlled pathways.<sup>2,7,8</sup> In this context, trying to identify impaired GR pathway(s)  
27 underlying GC-resistance and develop *de novo* a druggable molecule to restore  
28 responsiveness poses as a herculean task. A different approach to bypass GC-  
29 unresponsiveness of cancer cells would be to reposition alternatives from the pharmaceutical  
30 arsenal that are either approved or in late-stages of clinical trials for other GC-refractory  
31 inflammatory conditions. Given the emerging commonalities between inflammation and  
32 cancer, those alternatives might pose as latent substitutes of GCs' antiproliferative effect,  
33 awaiting in a "diamond-in-a-rough" state to be revisited in the context of cancer. This might  
34 decrease the pressure for natural selection of cancer cells that overcome the GC  
35 antiproliferative effects by deactivating their GR receptor and/or the GR-mediated pathways,  
36 the same way that prudent use of antibiotics or use of interchangeable antibiotics prevents  
37 the development of antibiotic-resistant microbe strains. Using GC-substitutes before ending-  
38 up prescribing GCs would also enable clinical oncologists to reserve the GC-based  
39 therapeutic options as a last-resort for aggressive tumors, without risking a possible induction  
40 of GC-resistance in earlier tumor stages.  
41  
42  
43  
44  
45  
46  
47  
48

49 To test this hypothesis we considered the mouse skin carcinogenesis system as our  
50 basal screening tool kit. Overall, the characteristics of our study system in terms of GC-  
51 sensitivity/GC-resistance and the underlying GR status are summarized in Table II. The  
52 model includes a GC-sensitive cell line C5N which retains a functional GR and can be used  
53  
54  
55  
56  
57  
58  
59  
60  
61  
62  
63  
64  
65

1  
2  
3 as the positive, comparative screening control cell line of the panel. The rest of the cell lines  
4 represent GC-resistant papillomas, squamous and spindle cells. In terms of localization, we  
5 additionally observed a GR accumulation in the nucleus during transition from squamous-to-  
6 spindle stages, resulting to a mixed cytoplasmic and nuclear signal in spindle cells. This  
7 unexpected and previously unreported finding, which was reconfirmed in *in vivo* mouse  
8 spindle skin cancer tumors, indicates the possible existence of an heterogenous population of  
9 GR isoforms and/or variants, some of which may have dominant negative function to the  
10 typical full-length isoforms. From the pathology point of view, this means that GR nuclear  
11 localization may not be a positive clinical indication for GC-responsiveness, as originally had  
12 been suggested <sup>37</sup>, especially given the fact that several dominant negative GR isoforms or  
13 splice variants that antagonize functional, full-length GR, and cause GC-unresponsiveness  
14 are also localized in the nucleus.<sup>1,2</sup>These issues will be clarified in future studies.

15  
16  
17  
18  
19 BrTaur, our first study case to be checked with our system, presents overlapping  
20 characteristics with GCs and is topically used in skin inflammatory conditions, such as acne  
21 vulgaris, instead of steroids <sup>13</sup>. It is well-tolerated and presents insignificant side-effects.<sup>13,15</sup>  
22 BrTaur surrogated for the antiproliferative effect on GC-sensitive and GC-resistant cells, thus  
23 providing the first evidence for its potential to be used interchangeably to GCs in the context  
24 of cancer, in the same concept they are currently clinically used interchangeably to GCs in  
25 the context of chronic inflammations and microbial infections. The fact that BrTaur efficiently  
26 synergizes with cisplatin to inhibit growth of GC-resistant cells further highlights its GC-  
27 mimicking therapeutic effect. The antiproliferative effect is strongly linked to the bromine  
28 moiety of the bromotaurine molecule and is mediated by inhibition of cell cycle in GC-  
29 resistant cells. The ability of BrTaur to produce a more consistent anticancer effect than  
30 taurine could be explained by the fact that the former is the ~~oxidizingrapidly drastie~~ form,  
31 while the latter is the maternal, reservoir substance, considered as a pro-drug. In detail,  
32 taurine is retained in several tissues, primarily in liver, and is recruited in tissues undergoing  
33 oxidative stress by topically-produced HOCl and HOBr to finally be ~~oxidizedreduced~~ to its  
34 ~~effectivedrastie~~ taurine haloamine derivatives. These scavenge the toxicity of the excess  
35 HOCl and HOBr and pick up the torch of immunologic responses at the lesion sites,  
36 preventing inflammation and exerting anti-microbial and ~~oxidizingantioxidant-like~~ properties<sup>13</sup>.  
37 In this respect, the inconsistent efficacy of taurine versus N-bromotaurine on the different cell  
38 lines of the mouse carcinogenesis system may be due to fluctuated micro-concentrations of  
39 HOBr in each different cell line milieu, thus resulting to corresponding fluctuations in the  
40 concentration of the active BrTaur finally being formed.

41  
42  
43  
44  
45  
46  
47  
48  
49  
50 It should be noted that overproliferation in our system, as in actual tumors, is  
51 associated with deregulation of several main pathways in addition to GR transactivation  
52 impairment.<sup>19</sup> These pathways, such as the ER $\alpha$  and AP-1 oncogenic pathways, crosstalk  
53  
54  
55  
56  
57  
58  
59  
60  
61  
62  
63  
64  
65

1  
2  
3 with GR since they are antagonized by its transrepression mode of action. Their progressive  
4 overactivation towards the aggressive stages in our system<sup>22,26,38</sup> implies a dysfunctional GR  
5 transrepression mode additionally to the demonstrated impairment of GR transactivation  
6 mode. Furthermore, the mixed cytoplasmic and nuclear signal detected in aggressive stages  
7 of skin cancer indicates the possible existence of a heterogeneous population of GR isoforms  
8 and/or variants, some of which may have dominant negative function to the typical full-length  
9 isoforms. This could be an additional reason for GR's inability to transactivate its targets and,  
10 thus, to subsequently mediate the antiproliferative effects of GCs in GC-resistant cells. This  
11 would mean that multiple factors causing GC-resistance are possibly accumulating towards  
12 the most aggressive stages. Therefore, our system must not be seen as a model dedicated to  
13 the study of a single GC-resistance cause. Rather, it should be cautiously used as a tool kit  
14 for performing preliminary screenings in order to discriminate the alternative agents with no  
15 antiproliferative action from the ones with the potential to restore antiproliferative response in  
16 GC-resistant cells.  
17  
18  
19  
20  
21

22 Notably, although skin cancers are primarily associated with impairment of the GR/GC  
23 axis, they are not treated with GCs. Thus our model is not proposed as a means to spot GC-  
24 substitutes against this cancer type. However, it is the demonstrated ability of this skin  
25 cancer-based artificial model to produce results that are extrapolated to several other types of  
26 epithelial cancers<sup>21</sup>, including the ones that are commonly treated with GCs, that gives this  
27 model an added value as an emerging generalized screening tool kit for identifying GC-  
28 substitutes. Using this basal screening tool, substances that are suspected, based on medical  
29 experience in the clinic, to have overlapping profiles with GCs could be confirmed as GC-  
30 substitutes before being repurposed for the management of cancer patients. Based on this  
31 screening tool, investigational N-bromotaurine was shown to act as a GC-substitute, while its  
32 effects were reproduced in cancer types that are commonly treated with GCs, such as the  
33 GC-resistant human breast and prostate cancer cell lines. Further confirmation of this anti-  
34 tumor effect in experimental animals in future studies could accelerate subsequent  
35 repositioning of BrTaur for the management of clinical cancer patients.  
36  
37  
38  
39  
40  
41

42 The point our approach highlights is that already-in-clinical-use compounds, able to  
43 consistently induce an antiproliferative phenotype in GC-resistant cells, even via molecular  
44 circuits which are currently as unknown to molecular biologists, as are unfamiliar to the GC-  
45 resistant cancer cells themselves, warrant to be unveiled and considered as possible GC-  
46 substitute therapeutic solutions. Analogous with what happens with newer generation  
47 antibiotics that catch the microbes unawares, the success of such compounds to startle  
48 cancer cells towards an antiproliferative direction may rely to their possible ability to act  
49 through pathways that the cancer cells have never been called to deactivate before in order  
50 to become aggressive. Such GC-substitutes may have the clinical potential to prolong  
51  
52  
53  
54  
55  
56  
57  
58  
59  
60  
61  
62  
63  
64  
65

1  
2  
3 disease free-survival, reduce tumor size, delay progression, mitigate side-effects and improve  
4 quality of life, in combination with well-established drugs, thus complying to the FDA's  
5 established guidelines on cancer clinical trial end-points.  
6 <http://www.fda.gov/downloads/Drugs/Guidances/ucm071590.pdf>.  
7

8 Last but not least, burning issues regarding BrTaur mechanism of action are awaiting  
9 to be thoroughly addressed in future studies. Potential ways for its systemic administration in  
10 the context of cancer therapeutics should also be explored. Anti-inflammatory effects of  
11 BrTaur are mediated by modification of the IkappaBalpha, an NF-kappaB inhibitor<sup>39</sup>. This  
12 interaction could also underlie BrTaur antiproliferative effects on GC-resistant cells, given that  
13 NF-kappaB stands in the cross-roads between inflammation and cancer<sup>40</sup> and is a crucial  
14 effector of GR-mediated tumor-suppressor effects<sup>2</sup>. Given the commonalities shared between  
15 anti-inflammatory and anti-cancer pathways, BrTaur may, at least in part, exert its anti-cancer  
16 action, in addition to its well-known anti-inflammatory properties<sup>13</sup> by targeting common  
17 networks underlying both pathological entities<sup>17,18</sup>. Comprehensive, high-throughput analyses  
18 of the molecular and cellular changes and the transcriptional programs alterations triggered  
19 upon BrTaur treatment using state-of-the-art, multiomics approaches are anticipated to shed  
20 more light on this issue in the future. The full range of BrTaur functions might extend beyond  
21 interfering with GR-mediated pathways, and is currently under investigation. The role of  
22 BrTaur in cancer emerges as a subject of fruitful research and poses as a mysterious "black  
23 box", the decoding of which might pave the way for next generation therapeutics.  
24  
25  
26  
27  
28  
29  
30

### 31 32 33 **ACKNOWLEDGEMENTS**

34 All authors have read the journal's authorship agreement and the manuscript has been  
35 reviewed and approved by all named authors. All authors have read the journal's policy on  
36 conflicts of interest and declare that there are no conflicts of interest. SL was supported by  
37 "IKY fellowships of excellence for postgraduate studies in Greece-Siemens program" given in  
38 terms of the settlement between the Greek Government and Siemens company. ES was  
39 funded by the "Scholarships Programs by the State Scholarships Foundation" in the  
40 framework of the Operational Program "Education and Life Long Learning" within the National  
41 Strategic Reference Framework. N-bromotaurine formulation was a donation of NASCO AD.  
42 Biotechnology Laboratory, for use in this preclinical research.  
43  
44  
45  
46  
47  
48  
49  
50  
51  
52  
53  
54  
55  
56  
57  
58  
59  
60  
61  
62  
63  
64  
65



## REFERENCES

1. Herr I, et al. Glucocorticoid cotreatment induces apoptosis resistance toward cancer therapy in carcinomas. *Cancer Res* 2003;63:3112-20.
2. Ramamoorthy S, Cidlowski JA. Exploring the molecular mechanisms of glucocorticoid receptor action from sensitivity to resistance. *Endocr Dev* 2013;24:41-56.
3. Budunova IV, et al. Glucocorticoid receptor functions as a potent suppressor of mouse skin carcinogenesis. *Oncogene* 2003;22:3279-87.
4. Chebotaev D, Yemelyanov A, Budunova I. The mechanisms of tumor suppressor effect of glucocorticoid receptor in skin. *Mol Carcinog* 2007;46:732-40.
5. Latorre V, et al. Selective ablation of glucocorticoid receptor in mouse keratinocytes increases susceptibility to skin tumorigenesis. *J Invest Dermatol* 2013;133:2771-9.
6. Herr I, Pfizenmaier J. Glucocorticoid use in prostate cancer and other solid tumours: implications for effectiveness of cytotoxic treatment and metastases. *Lancet Oncol* 2006;7:425-30.
7. Lambrou GI, et al. Glucocorticoid and proteasome inhibitor impact on the leukemic lymphoblast: multiple, diverse signals converging on a few key downstream regulators. *Mol Cell Endocrinol* 2012;351:142-51.
8. Copland JA, et al. Sex steroid receptors in skeletal differentiation and epithelial neoplasia: is tissue-specific intervention possible? *Bioessays* 2009;31:629-41.
9. Spiegelman VS, et al. Resistance of transformed mouse keratinocytes to growth inhibition by glucocorticoids. *Mol Carcinog* 1997;20:99-107.
10. Piovan E, et al. Direct reversal of glucocorticoid resistance by AKT inhibition in acute lymphoblastic leukemia. *Cancer Cell* 2013;24:766-76.
11. Allison M. NCATS launches drug repurposing program. *Nat Biotechnol* 2012;30:571-2.
12. Barnes PJ, Adcock IM. Glucocorticoid resistance in inflammatory diseases. *Lancet* 2009;373:1905-17.
13. Marcinkiewicz J, Kontny E. Taurine and inflammatory diseases. *Amino Acids* 2014;46:7-20.
14. Islambulchilar M, et al. Taurine attenuates chemotherapy-induced nausea and vomiting in acute lymphoblastic leukemia. *Amino Acids* 2015;47:101-9.
15. Marcinkiewicz J, et al. Topical taurine bromamine, a new candidate in the treatment of moderate inflammatory acne vulgaris: a pilot study. *Eur J Dermatol* 2008;18:433-9.
16. Gottardi W, Nagl M. N-chlorotaurine, a natural antiseptic with outstanding tolerability. *J Antimicrob Chemother* 2010;65:399-409.
17. Wogan GN, et al. Infection, inflammation and colon carcinogenesis. *Oncotarget* 2012;3:737-8.
18. Rayburn ER, Ezell SJ, Zhang R. Anti-Inflammatory Agents for Cancer Therapy. *Mol Cell Pharmacol* 2009;1:29-43.
19. Zoumpourlis V, et al. Alterations in signal transduction pathways implicated in tumour progression during multistage mouse skin carcinogenesis. *Carcinogenesis* 2003;24:1159-65.
20. Skourti E, et al. Progression of mouse skin carcinogenesis is associated with the orchestrated deregulation of miR-200 family members, miR-205 and their common targets. *Mol Carcinog* 2015.
21. Balmain A, Yuspa SH. Milestones in skin carcinogenesis: the biology of multistage carcinogenesis. *J Invest Dermatol* 2014;134:E2-7.
22. Logotheti S, et al. Progression of mouse skin carcinogenesis is associated with increased ERalpha levels and is repressed by a dominant negative form of ERalpha. *PLoS One* 2012;7:e41957.
23. Olszanecki R, et al. The role of heme oxygenase-1 in down regulation of PGE2 production by taurine chloramine and taurine bromamine in J774.2 macrophages. *Amino Acids* 2008;35:359-64.

- 1
- 2
- 3 24. Daskalos A, et al. Global DNA hypomethylation-induced DeltaNp73 transcriptional
- 4 activation in non-small cell lung cancer. *Cancer Lett* 2011;300:79-86.
- 5 25. Karakaidos P, et al. Overexpression of the replication licensing regulators hCdt1 and
- 6 hCdc6 characterizes a subset of non-small-cell lung carcinomas: synergistic effect
- 7 with mutant p53 on tumor growth and chromosomal instability--evidence of E2F-1
- 8 transcriptional control over hCdt1. *Am J Pathol* 2004;165:1351-65.
- 9 26. Papassava P, et al. Overexpression of activating transcription factor-2 is required for
- 10 tumor growth and progression in mouse skin tumors. *Cancer Res* 2004;64:8573-84.
- 11 27. Solakidi S, Psarra AM, Sekeris CE. Differential distribution of glucocorticoid and
- 12 estrogen receptor isoforms: localization of GRbeta and ERalpha in nucleoli and
- 13 GRalpha and ERbeta in the mitochondria of human osteosarcoma SaOS-2 and
- 14 hepatocarcinoma HepG2 cell lines. *J Musculoskelet Neuronal Interact* 2007;7:240-5.
- 15 28. Logotheti S, et al. Sp1 binds to the external promoter of the p73 gene and induces the
- 16 expression of TAp73gamma in lung cancer. *FEBS J* 2010;277:3014-27.
- 17 29. Vlahopoulos S, et al. Recruitment of the androgen receptor via serum response factor
- 18 facilitates expression of a myogenic gene. *J Biol Chem* 2005;280:7786-92.
- 19 30. Mattern J, Buchler MW, Herr I. Cell cycle arrest by glucocorticoids may protect normal
- 20 tissue and solid tumors from cancer therapy. *Cancer Biol Ther* 2007;6:1345-54.
- 21 31. Samuelsson MK, et al. p57Kip2, a glucocorticoid-induced inhibitor of cell cycle
- 22 progression in HeLa cells. *Mol Endocrinol* 1999;13:1811-22.
- 23 32. Ayroldi E, Riccardi C. Glucocorticoid-induced leucine zipper (GILZ): a new important
- 24 mediator of glucocorticoid action. *FASEB J* 2009;23:3649-58.
- 25 33. Kim T, Kim AK. Taurine enhances anticancer activity of cisplatin in human cervical
- 26 cancer cells. *Adv Exp Med Biol* 2013;776:189-98.
- 27 34. Zhang X, et al. Taurine induces the apoptosis of breast cancer cells by regulating
- 28 apoptosis-related proteins of mitochondria. *Int J Mol Med* 2015;35:218-26.
- 29 35. Martin-Sabroso C, et al. Overcoming glucocorticoid resistances and improving
- 30 antitumor therapies: lipid and polymers carriers. *Pharm Res* 2015;32:968-85.
- 31 36. Karmakar S, Jin Y, Nagaich AK. Interaction of glucocorticoid receptor (GR) with
- 32 estrogen receptor (ER) alpha and activator protein 1 (AP1) in dexamethasone-
- 33 mediated interference of ERalpha activity. *J Biol Chem* 2013;288:24020-34.
- 34 37. Antakly T, Thompson EB, O'Donnell D. Demonstration of the intracellular localization
- 35 and up-regulation of glucocorticoid receptor by in situ hybridization and
- 36 immunocytochemistry. *Cancer Res* 1989;49:2230s-2234s.
- 37 38. Zoumpourlis V, et al. High levels of phosphorylated c-Jun, Fra-1, Fra-2 and ATF-2
- 38 proteins correlate with malignant phenotypes in the multistage mouse skin
- 39 carcinogenesis model. *Oncogene* 2000;19:4011-21.
- 40 39. Tokunaga S, Kanayama A, Miyamoto Y. Modification of IkappaBalpha by taurine
- 41 bromamine inhibits tumor necrosis factor alpha-induced NF-kappaB activation.
- 42 *Inflamm Res* 2007;56:479-86.
- 43 40. Karin M. NF-kappaB as a critical link between inflammation and cancer. *Cold Spring*
- 44 *Harb Perspect Biol* 2009;1:a000141.
- 45
- 46
- 47
- 48
- 49
- 50
- 51
- 52
- 53
- 54
- 55
- 56
- 57
- 58
- 59
- 60
- 61
- 62
- 63
- 64
- 65

## FIGURE LEGENDS

**Figure 1:** Estimation of responsiveness of cell lines of the mouse skin carcinogenesis model to GCs (dexamethasone) by crystal violet assays. **(a)** In the representative time point of 48h, the ~~percentage~~ number of cells drastically decreases proportional to dexamethasone concentration in comparison with the untreated cells in the C5N cell line (expressed as ratio to untreated cells). In contrast, there is no change in cell numbers of dexamethasone-treated P6, B9, A5 and CarB cells compared to their corresponding untreated controls, in any of the concentrations tested. **(b)** The profile of the antiproliferative action of GCs on the GC-sensitive C5N cells over time, for each of the tested dexamethasone concentrations in comparison to a selected GC-resistant cell line P6. The experiments were performed in triplicates.

**Figure 2:** GR is translocated in nucleus during transition from squamous to spindle stage of skin carcinogenesis. **(a)** GR protein expression levels of total (tGR), cytoplasmic (cGR) and nuclear (nGR) extracts of the mouse skin carcinogenesis model. **(b)** ~~Quantification of~~ Western blot results indicates a switch in the cytoplasmic-to-nuclear GR ratio (cGR-to-nGR) during transition from squamous to spindle stage. **(c)** Immunocytochemistry analysis of the panel of mouse skin carcinogenesis model with anti-GR antibody revealed cytoplasmic staining in C5N, P6 and B9 cells, and mixed cytoplasmic and nuclear staining in A5 and CarB cells. The black arrows indicate GR-stained nuclei. These immunocytochemical patterns were rather uniform in the above mentioned cell lines. **(d)** The immunofluorescence GR signal is cytoplasmic in the squamous B9 cells, but nuclear in the spindle A5 cells. **(e)** Immunohistochemistry using anti-GR antibody in paraffin-embedded tissues isolated from the papilloma, squamous and spindle stage of the same chemically-induced tumor in one mouse revealed higher number of GR-stained nuclei in spindle cells in comparison with the corresponding papilloma and squamous stage. Each figure represents a 200x magnitude, whereas the upper-right boxes in each figure represent a 400x magnitude. The black boxes represent the magnified area. The black arrows indicate GR-stained nuclei.

**Figure 3:** GR is DNA binding-competent but transactivation-incompetent in GC-resistant cell lines of the mouse skin carcinogenesis model. **(a)** Electrophoretic mobility shift assay in the GC-responsive C5N revealed binding activity of GR to glucocorticoid responsive elements (GRE) only upon dexamethasone (C5N+dex) treatment. **(b)** EMSA assay for GR using nuclear extracts demonstrated binding activity of GR to glucocorticoid responsive elements (GRE) of the GC-unresponsive P6, B9, A5 and CarB cells in the absence of dexamethasone signal. DNA binding increases directly proportional to the demonstrated nuclear GR protein

Formatted: Font: Not Bold

Formatted: Justified

1  
2  
3 levels towards more aggressive cell lines. Specificity of the EMSA reaction is confirmed by  
4 supershift reactions in A5 (lane 6) cells using anti-GR antibody. (c) Luciferase assays in the  
5 GC-sensitive and the GC-resistant cells of the mouse skin carcinogenesis model  
6 co-transfected with the 17m-GRE-G-Luc, in dexamethasone absence (-dex) or presence (+dex).  
7 Luciferase expression is significantly induced (One asterisk (\*) denotes p <0.05) only in the  
8 GC-sensitive C5N cells upon dexamethasone treatment. Error bars represent the standard  
9 error of the mean. Two-tailed p values are derived from independent t-tests. Three  
10 biological replicates were available for each experiment. (d) Box plots demonstrating the  
11 transcription induction of GILZ under dexamethasone treatment in Q-PCR estimation of GILZ  
12 levels in the GC-sensitive and the GC-resistant cell lines before (-dex) and after (+dex)  
13 dexamethasone treatment, estimated by qPCR. The relative quantification (RQ) values in  
14 log<sub>10</sub> are shown. For each cell line, the untreated control was used as calibrator. The  
15 housekeeping gene beta-2 microglobulin was used as an internal control of mRNA Q-PCR  
16 expression. The experiments were performed in triplicates. (e) Same as 3d, for p57<sup>KIP2</sup> mRNA  
17 levels. In both genes, significant induction is only observed in C5N cells (indicated by star).  
18 RQ: relative quantification value.

Formatted: Font: (Default) Arial

Formatted: English (United States)

27  
28 **Figure 4:** Estimation of the antiproliferative response of the GC-sensitive and the GC-  
29 resistant cell lines to N-bromotaurine by proliferation assays. (a) In the representative time  
30 point of 48h, the percentage number of cells drastically decreases in comparison with the  
31 corresponding untreated control cells for all cell lines of the study model (expressed as ratio  
32 to untreated cells). (b) Comparative treatment of the cells with the maternal substance taurine  
33 did not affect mouse skin cancer cell proliferation in a significant and consistent manner,  
34 implying that bromination of the taurine is the crucial factor for the consistent antiproliferative  
35 effect on cells. (c) The profile of the antiproliferative action of N-bromotaurine on the GC-  
36 resistant GC-resistant prostate cancer PC3. (d) Same as 4c. for the human GC-resistant  
37 prostate cancer MDA-MB-231. The experiments were performed in triplicates.

43  
44 **Figure 5:** Comparison of the antiproliferative response of the aggressive GC-resistant cells to  
45 GCs versus N-bromotaurine. (a) proliferation assays on CarB cells treated with  
46 dexamethasone reveal lack of significant antiproliferative response of CarB upon addition of  
47 GCs over time, as evidenced by the OD measurements. (b) In contrast, proliferation assays  
48 on CarB cells treated with N-bromotaurine instead of dexamethasone reveal restoration of  
49 antiproliferative response of CarB cells by N-bromotaurine over time. The restoration of  
50 antiproliferative response is statistically significant ~~potent~~ in the 250µM concentration, after 48  
51 and 72 hours of N-bromotaurine treatment. Three independent experiments were performed,

1  
2  
3 each in triplicate. ~~Mean values were significantly different from those of the untreated controls~~  
4 ~~in the N-bromotaurine treated cells, but not in the dexamethasone treated cells.~~ The  
5 means±SEM values are shown in the graphs. **(c)** FACS analysis of N-bromotaurine-treated  
6 CarB cells (CarB + BrTaur) compared with dexamethasone-treated CarB cells (CarB + dex)  
7 and untreated CarB cells (CarB). BrTaur, at concentrations of 125µM and 250µM, ~~increased~~  
8 the number of cells in G0/G1 phase; whereas at the high concentration of 500µM, BrTaur  
9 drastically decreased both G0/G1 and G2/M phases. Dexamethasone, at 10<sup>-7</sup>M concentration  
10 failed to significantly affect the number of cells in G1/G0 phase. Corresponding summary  
11 graphs for each phase of the cell cycle (means±SEM from 3 independent FACS analyses  
12 measurements) derived by comparison of untreated CarB cells each of the dexamethasone-  
13 treated, 125µM BrTaur-treated, 250µM BrTaur-treated and 500µM BrTaur-treated CarB cells,  
14 ~~using t test.~~ **(d-f)** 250µM BrTaur-treated and 500µM BrTaur-treated CarB cells synergized  
15 efficiently with 2.9 cisplatin (cis) after 48hours of BrTaur plus cisplatin combination therapy as  
16 **(d)** pre-treatment (BrTaur + cis), **(e)** concurrent treatment (cis/BrTaur) or **(f)** post-treatment (cis  
17 + BrTaur) ~~, t test, p value <0.05.~~ Results are flagged with no asterisk when p-value is more  
18 than 0.05, and with ~~two~~ asterisks when the p-value is less than 0.0015. (See text for details  
19 on treatment schemes of 5d-f).  
20  
21  
22  
23  
24  
25  
26  
27  
28  
29  
30  
31  
32  
33  
34  
35  
36  
37  
38  
39  
40  
41  
42  
43  
44  
45  
46  
47  
48  
49  
50  
51  
52  
53  
54  
55  
56  
57  
58  
59  
60  
61  
62  
63  
64  
65

Formatted: English (United States)

**N-bromotaurine surrogates for loss of antiproliferative response and enhances cisplatin efficacy in cancer cells with impaired glucocorticoid receptor**

Stella Logotheti<sup>1,7</sup>, Nikolas Khoury<sup>1</sup>, Spiros A. Vlahopoulos<sup>2</sup>, Elena Skourti<sup>1</sup>, Dimitra Papaevangelou<sup>1</sup>, Triantafyllos Liloglou<sup>3</sup>, Vassilis Gorgoulis<sup>4</sup>, Irina Budunova<sup>5</sup>, Anthony M. Kyriakopoulos<sup>6</sup>, Vassilis Zoumpourlis<sup>1\*</sup>

<sup>1</sup>Biomedical Applications Unit, Institute of Biology, Medicinal Chemistry and Biotechnology, National Hellenic Research Foundation, 48 Vassileos Constantinou Avenue, 116 35 Athens, Greece.

<sup>2</sup>Horemio Research Institute, First Department of Pediatrics, "Aghia Sophia" Children's Hospital, National and Kapodistrian University of Athens, Athens, Greece.

<sup>3</sup>University of Liverpool, Department of Molecular and Clinical Cancer Medicine, 200 London Road, Liverpool L3 9TA, UK

<sup>4</sup>Laboratory of Histology-Embryology, Molecular Carcinogenesis Group, Medical School, National and Kapodistrian University of Athens, Athens, Greece.

<sup>5</sup>Department of Dermatology, Northwestern University, Chicago, IL, USA.

<sup>6</sup>Nasco AD, Biotechnology Laboratory, 11th Sachtouri str., Piraeus, Greece.

<sup>7</sup>Department of Biotechnology, Agricultural University of Athens, Athens, Greece

\* Corresponding author

Tel: 30-10-7273730

Fax: 30-10-7273677

e-mail: vzub@eie.gr

Running title : Repurposing BrTaur in GC-resistant cancers

Keywords: GR; glucocorticoid resistance; N-bromotaurine; skin carcinogenesis; drug repurposing

Abbreviations: GC: glucocorticoid; GR: glucocorticoid receptor; GRE: glucocorticoid receptor element; NSAID: non-steroid anti-inflammatory drug; BrTaur: N-bromotaurine; CITaur: N-chlorotaurine; EMSA: electrophoretic mobility shift assay; FACS: fluorescence-activated cell sorting; qRT-PCR: quantitative Real-Time-Polymerase Chain Reaction.

## ABSTRACT

1  
2  
3  
4  
5  
6  
7  
8  
9  
10  
11  
12  
13  
14  
15  
16  
17  
18  
19  
20  
21  
22  
23  
24  
25  
26  
27  
28  
29  
30  
31  
32  
33  
34  
35  
36  
37  
38  
39  
40  
41  
42  
43  
44  
45  
46  
47  
48  
49  
50  
51  
52  
53  
54  
55  
56  
57  
58  
59  
60  
61  
62  
63  
64  
65

Glucocorticoids (GCs) are frequently used in anticancer combination regimens; however, their continuous use adds selective pressure on cancer cells to develop GC-resistance via impairment of the glucocorticoid receptor (GR), therefore creating a need for GC-alternatives. Based on the drug repurposing approach and the commonalities between inflammation and neoplasia, drugs that are either in late-stage clinical trials and/or already marketed for GC-refractory inflammatory diseases, could be evaluated as GC-substitutes in the context of cancer. Advantageously, unlike new molecular entities currently being *de novo* developed to restore GC-responsiveness of cancer cells, such drugs have documented safety and efficacy profile, which overall simplifies their introduction in clinical cancer trials. In this study, we estimated the potential of a well-established, multistage, cell line-based, mouse skin carcinogenesis model to be exploited as an initial screening tool for unveiling covert GC-substitutes. First, we categorized the cell lines of this model to GC-sensitive and GC-resistant, in correlation with their corresponding GR status, localization and functionality. We found that GC-resistance starts in papilloma stages, due to a dysfunctional GR, which is overexpressed, DNA binding-competent, but transactivation-incompetent in papilloma, squamous and spindle stages of the model. Then, aided by this tool, we evaluated the ability of N-bromotaurine, a naturally-occurring, small-molecule, NSAID which is under consideration for use interchangeably/in replacement to GCs in skin inflammations, to restore antiproliferative response of GC-resistant cancer cells. Unlike GCs, N-bromotaurine inhibited cell-cycle progression in GC-resistant cancer cells and efficiently synergized with cisplatin, thus indicating a potential to be exploited instead of GCs against cancer.

## INTRODUCTION

1  
2  
3  
4  
5  
6  
7  
8  
9  
10  
11  
12  
13  
14  
15  
16  
17  
18  
19  
20  
21  
22  
23  
24  
25  
26  
27  
28  
29  
30  
31  
32  
33  
34  
35  
36  
37  
38  
39  
40  
41  
42  
43  
44  
45  
46  
47  
48  
49  
50  
51  
52  
53  
54  
55  
56  
57  
58  
59  
60  
61  
62  
63  
64  
65

Glucocorticoids (GCs) are steroid hormones which inhibit tumor cell proliferation, mitigate chemotherapy side effects and enhance efficiency of anticancer agents<sup>1,2</sup>. They are frequently included in combination anticancer therapies, either as palliative agents against chemotherapy-induced-nausea-and-vomiting or as antiproliferative agents. Their effects are mediated by the glucocorticoid receptor (GR). GC binds to GR which, following dissociation from a cytoplasmic chaperone/co-chaperone complex, translocates to the nucleus, homodimerizes and regulates gene expression. GR transactivates or transrepresses genes by direct binding to GREs (glucocorticoid responsive elements), by tethering itself to other transcription factors apart from DNA binding, or in a composite manner by both direct GRE binding and interactions with transcription factors bound to neighboring sites (reviewed by Ramamoorthy et al<sup>2</sup>). Thus, a functional GR elicits tumor-suppressive events in a pleiotropic manner, through a plethora of mechanisms and crucial pathways.<sup>3-5</sup>

Theoretically, the clinical benefits demonstrated by the long-term experience on GCs, combined with the tumor-suppressive nature of GR, offer a strong alibi for their routine use in cancer therapeutics (e.g. prostate cancer, breast cancer, leukemia), as evidenced by the increasing number of GC-containing combination regimens, both established and investigational. Nevertheless, GC cotreatment often induces resistance towards cancer therapy<sup>1,6</sup> thus raising concerns regarding the tendency of GC-sensitive cancer cells to develop resistance upon frequent GC use. Mechanistically, this tendency is attributed to the pleiotropic nature of GR *per se*. GR's pleiotropy becomes a double-edged sword, since cancer cells have, at their disposal, as many potentials to overcome GR's antiproliferative barrier and achieve GC-resistance, as is the plethora of underlying GR-mediated antiproliferative pathways they can defuse one way or another. For neutralizing GR antiproliferative effects, cancer cells exploit several strategies, which in several cases simultaneously co-exist in a cancer cell (e.g. reduced GR expression, reduced DNA binding ability, GR mutations and polymorphisms, co-expression of dominant negative GR isoforms, impairment of transrepression mode et.c.).<sup>2,7,8</sup> GC-unresponsiveness by GR impairment may start as early as the benign stages, highlighting that inactivation of GC/GR axis is a selective advantage in order for a cancer cell to surpass the antiproliferative break and continue its tumorigenic march towards aggressive stages.<sup>9</sup>

This overall necessitates alternatives restoring and/or surrogating for GCs' antiproliferative effects.<sup>2,10</sup> To this end, innovative synthetic molecules are being developed by academia, aiming to re-activate GR-mediated antiproliferative pathways and restore GC-responsiveness of cancer cells<sup>10</sup>. If they successfully pass clinical trials, they will eventually find their way to the bedside. But this established bench-to-bedside pipeline is not an one-way street. The recently framed concept of drug repurposing suggests evaluating suitability of



1  
2  
3  
4  
5  
6  
7  
8  
9  
10  
11  
12  
13  
14  
15  
16  
17  
18  
19  
20  
21  
22  
23  
24  
25  
26  
27  
28  
29  
30  
31  
32  
33  
34  
35  
36  
37  
38  
39  
40  
41  
42  
43  
44  
45  
46  
47  
48  
49  
50  
51  
52  
53  
54  
55  
56  
57  
58  
59  
60  
61  
62  
63  
64  
65

known drugs for use in new indications<sup>11</sup>. Implementing this concept in the issue of GC-resistance, we postulate that drugs which are already in late stages of clinical trials or approved for indications other than cancer may be latent GC-substitutes, able to imitate aspects of the GC therapeutic profile. These hypothetical latent GC-substitutes might be competent to either restore the antiproliferative phenotypes in GC-resistant cells; or to be used interchangeably to GCs, in order to reduce the selective pressure exerted by continuous use of GCs on GC-sensitive cells, thus preventing/delaying their clonal expansion to GR-impaired and, hence, GC-resistant cells. A clinical advantage of the proposed approach is that these candidate substances are actually closer to the bedside than they are to the bench, since they have a more characterized efficacy and safety profile, in terms of their documentation for other therapeutic indications. This is translated to both faster filing and regulatory approval procedures and to reduced financial costs to develop these substances as anticancer agents, compared to starting the anticancer drug research-and-development workflow from scratch, i.e. by developing New Molecular Entities (NMEs, defined by FDA as experimental substances without precedent among regulated and approved drug products).<sup>11</sup>

Except for anticancer agents, GCs are also common anti-inflammatory agents. In fact, their use against inflammations historically preceded their use against neoplasias. GC-resistance is a frequent problem in inflammations as well, and drugs are being developed in replacement of GC-containing anti-inflammatory regimens.<sup>12</sup> Emerging GC-substitutes that are currently in the investigational clinical setting for inflammation management include, but are not limited to, the NSAID (Non-Steroid Anti-Inflammatory Drug) taurine haloamine derivatives, mainly N-bromotaurine (BrTaur) and N-chlorotaurine (ClTaur). These are generated by eosinophils and neutrophils at a site of inflammation and exert potent anti-inflammatory properties. Other common features shared with GCs is their naturally-occurring and small-molecule nature and their immunomodulatory and antimicrobial properties<sup>13</sup>. Another common characteristic is the potential to ameliorate chemotherapy-induced nausea and vomiting, since their maternal substance, i.e. the non-essential amino acid taurine, which is orally administered as a pro-drug in order to be converted to the haloamine derivative at the site of inflammation, was recently proven clinically capable of such an effect in leukemic patients.<sup>14</sup> Advantageously, taurine haloamines have shown good efficacy, tolerance and insignificant toxic effects upon topical use on clinical patients who are refractory to conventional GC-based anti-inflammatory therapies<sup>13,15,16</sup>. Based on the association between chronic inflammatory diseases and neoplasias,<sup>17,18</sup> we postulated that a drug which exerts overlapping features and common therapeutic indications with GCs and is able to surrogate for GCs in GC-resistant inflammations may be able to surrogate for the GCs' antiproliferative function in GC-resistant cancer cells as well.

1  
2  
3  
4  
5  
6  
7  
8  
9  
10  
11  
12  
13  
14  
15  
16  
17  
18  
19  
20  
21  
22  
23  
24  
25  
26  
27  
28  
29  
30  
31  
32  
33  
34  
35  
36  
37  
38  
39  
40  
41  
42  
43  
44  
45  
46  
47  
48  
49  
50  
51  
52  
53  
54  
55  
56  
57  
58  
59  
60  
61  
62  
63  
64  
65

As a springboard for testing this hypothesis, we took advantage of our long-term experience on a well-established mouse model of skin carcinogenesis.<sup>19</sup> This comprises of a series of cell lines which represent different stages of mouse skin tumor progression and are categorized on the basis of increasing aggressiveness to immortalized keratinocytes (C5N), benign papillomas (P6), malignant squamous carcinomas (B9), and highly invasive spindle cells (A5, CarB).<sup>19</sup> The B9:A5 pair represents the clonal expansion from squamous to spindle stages. The model has been developed in Dr. A. Balmain's lab and has been thoroughly reviewed<sup>18</sup> and described previously.<sup>20</sup> Briefly, in order to obtain these cell lines, each of which represent the initiation, promotion or progression stages of skin carcinogenesis, a chemical carcinogenesis protocol on mice was applied. The normal epidermis of mice or normal epithelial mouse cells were treated with a single dose of the polycyclic aromatic hydrocarbon 7,12 dimethylbenz[a]anthracene (DMBA), followed by weekly applications of the phorbol ester 12-O-tetradecanoylphorbol-13-acetate (TPA). This led to the development of numerous benign papillomas, some of which progressed to malignant squamous cell carcinomas several weeks after the first exposure to carcinogens and cell lines were produced from these tumors. Overall, this model poses the following advantages: a) it is multistage, meaning that it simulates the step-wise manner by which a tumor initiates, promotes and progresses, b) it is coherent, since cell lines have been derived in a consistent manner following a meticulous chemical carcinogenesis protocol, c) although skin-tissue based, it further applies to almost all epithelial cancers.<sup>21</sup> Furthermore, the fact that the model is skin tissue-based facilitates our analysis, because skin cancer is a traditional field where the mechanisms of GR function in correlation to GC-responsiveness have been adequately studied.<sup>4,5,9</sup> Therefore, although our model has never been characterized before in terms of GC-responsiveness, it stood a good chance to faithfully mirror or even complement previous robust findings.

First, we characterized our system in terms of antiproliferative response to GCs. Then, we correlated this responsiveness to the underlying GR expression status, localization and functionality. Finally, we checked the ability of BrTaur to bypass GC-resistance of cancer cells either alone or in combination with cisplatin.

## **MATERIALS AND METHODS**

### ***Cells and culture conditions***

Mouse cell lines of the mouse skin carcinogenesis model have been produced and obtained by Dr. Allan Balmain. All human cell lines used were obtained by American Type Culture Collection (ATCC). Cells were cultured as previously described.<sup>22</sup> The preparation<sup>23</sup> and use

1  
2  
3  
4  
5  
6  
7  
8  
9  
10  
11  
12  
13  
14  
15  
16  
17  
18  
19  
20  
21  
22  
23  
24  
25  
26  
27  
28  
29  
30  
31  
32  
33  
34  
35  
36  
37  
38  
39  
40  
41  
42  
43  
44  
45  
46  
47  
48  
49  
50  
51  
52  
53  
54  
55  
56  
57  
58  
59  
60  
61  
62  
63  
64  
65

of BrTaur is covered by licensing agreement. The in-house formulation was donated by NASCO AD Biotechnology Laboratory for preclinical research purposes.

### ***Proliferation assays***

Collectively, 2250 cells per well were seeded in 96-well plates. After cells were attached, the first measurement was taken. This time point is called 0 hours. At this point, 24h after seeding, dexamethasone ( $10^{-9}$  –  $10^{-6}$ M, from a stock of  $10^{-3}$ M dexamethasone diluted in ethanol), BrTaur (25 $\mu$ M-250 $\mu$ M from a stock of 4mM BrTaur) or taurine (5-50mM from a stock of 200mM taurine diluted in water) was added and measurements were taken after 24, 48 and 72h. For co-treatment experiments, cells were treated with either  $10^{-7}$ M dexamethasone or BrTaur (125, 250 or 500 $\mu$ M) 24-hours prior, con-currently with or 24-hours post cisplatin treatment. Untreated cells were used as controls. Following treatments, cells were fixed with 100% methanol and, then, crystal violet solution was added to each well. After a 10-minute incubation in room temperature, each well was washed 3 times with 200 $\mu$ L water, and plates were incubated on a shaker for 45min. Optical Density (OD) was measured at 595nm using a Tecan reader. The data was transferred to Microsoft Excel and analyzed. Background absorbance was corrected using triplicate sets of wells containing medium only (no cells) and crystal violet reagent as per experimental well. Three independent experiments were performed and each one of them included a triplicate value set.

### ***RNA extraction, cDNA synthesis and qRT-PCR analysis***

mRNA extraction, cDNA synthesis and quantitative real-time PCR was conducted as previously described.<sup>24</sup> Primers used appear in Table I.

### ***Preparation of cell lysates and Western blot analysis***

Total, cytoplasmic and nuclear cell lysates were prepared as previously described.<sup>25</sup> The primary antibody was an in-house anti-GR rabbit polyclonal antibody, clone 2F8, against aminoacids 305-427 of the N-terminal domain (kindly provided by Dr. M.N. Alexis), in a 1:500 dilution. Primary anti-beta-actin antibody in a 1:1000 dilution was used as a loading control. The secondary antibody was a mouse anti-rabbit antibody (Santa Cruz Biotechnology, Santa Cruz, CA) in a 1:1000 dilution.

### ***Two-stage chemical carcinogenesis protocol***

Tumors induced on mouse skin following a chemical carcinogenesis protocol were fixed and paraffin-embedded. Slides carrying formalin-fixed paraffin-embedded (FFPE) mouse skin papilloma and squamous and spindle tumors were prepared as previously described.<sup>22</sup> In

1 vivo experiments were performed in the in-house authorized animal house. Experiments  
2 complied with the Protocol on the Protection and Welfare of Animals, as obliged by the rules  
3 of the National Hellenic Research Foundation, the regulations of the National Bioethics  
4 Committee and the article 3 of the presidential decree 160/1991 (in line with 86/609/EEC  
5 directive) regarding the welfare of experimental animals.  
6  
7

### 8 9 10 ***Immunohistochemical and immunocytochemical staining***

11 Immunohistochemical staining on FFPE sections was performed as described earlier.<sup>26</sup> The  
12 sections were stained with anti-GR, clone 2F8, in a 1:10 dilution. For the  
13 immunocytochemistry staining with anti-GR antibody 2F8, we followed the same procedure,  
14 incubation periods and reagents, by omitting the deparaffinization step.  
15  
16  
17

### 18 19 20 ***Immunofluorescence staining***

21 Cells were grown and fixed on coverslips and where subjected to immunofluorescence  
22 staining as previously described.<sup>27</sup> The slides were incubated with primary antibody anti-GR,  
23 clone M-20 (Santa Cruz Biotechnology, Santa Cruz, CA) in a 1:50 dilution. The secondary  
24 antibody was anti-rabbit FITC-conjugated (Jackson Laboratory, Bar Harbor, Maine, USA)  
25 diluted in 1:100.  
26  
27  
28  
29

### 30 31 32 ***Electrophoretic Mobility Shift assay***

33 Annealed oligonucleotides for the *human metallothionin IIA* Glucocorticoid Responsive  
34 Element (5'-TGGTACACTGTGTCCTGAATTCA-3' and 5'-  
35 TGAATTCAGGACACAGTGTACCA-3') were end-labeled with  $\gamma^{32}\text{P}$ -ATP using T4-  
36 polynucleotide kinase and the reaction products were purified on a 8% polyacrylamide gel.  
37 DNA binding reactions were performed as previously described.<sup>28</sup> For the supershift control  
38 experiment, the primary polyclonal antibody anti-GR 10-10 (kindly provided by Dr. M. Alexis)  
39 was used.  
40  
41  
42  
43  
44  
45

### 46 47 ***Plasmids, transfections and luciferase reporter assay***

48 A luciferase plasmid carrying GRE sequences (17m-GRE-G-Luc), as well as a control vector  
49 carrying no GRE binding site (tata-pG13Luc) described previously<sup>29</sup> were used for  
50 transfections. Where indicated, cells were incubated with dexamethasone and transfected  
51 with by the calcium phosphate method, as described previously<sup>7</sup>. The luciferase activity was  
52 measured using a luminometer and was normalized for transfection efficiency with the  $\beta$ -  
53 galactosidase activity.  
54  
55  
56  
57  
58  
59

### 60 ***FACS analysis***

61  
62  
63  
64  
65

1 Cells were harvested, trypsinized and centrifuged at 1,000rpm for 5min, at room temperature.  
2 The pellet was resuspended in 500µL PBS, fixed with 80% ethanol, vortexed, and stained  
3 with propidium iodide (50µg/mL), in the presence of 5mmol/L MgCl<sub>2</sub> and 10µg/mL RNase A in  
4 10mmol/L Tris-HCl (pH 7.5). DNA content was analyzed on a FACSCalibur (Becton  
5 Dickinson) using the Modfit software.  
6  
7  
8  
9

### 10 **Statistical analysis**

11 Data are expressed as mean±SD. Each experiment was performed in triplicates. Then, the  
12 triplicate set values of three independent experiments were analyzed. For statistical analyses  
13 of proliferation assays results, ANOVA utilising Dunetts' T3 post-hoc analysis was applied.  
14 QPCR results were evaluated using Mann-Whitney's test. Luciferase assays were analyzed  
15 using independent student's t-tests. P values of less than 0.05 were considered significant.  
16  
17  
18  
19  
20  
21

## 22 **RESULTS**

### 23 ***The antiproliferative effect of GCs is lost in the promotion and progression stages of*** 24 ***mouse skin carcinogenesis***

25 Our first priority was to explore the GC antiproliferative effect on the cell lines of our system.  
26 GC effect ranges from proliferative in very low concentrations, to cytostatic/antiproliferative in  
27 more physiological concentrations and cytotoxic/apoptotic in higher concentrations.<sup>30</sup> To  
28 monitor GC effect on our system, we treated cells with a range of dexamethasone  
29 concentrations previously demonstrated to show antiproliferative effects on mouse  
30 keratinocytes (10<sup>-9</sup>M - 10<sup>-6</sup>M),<sup>9</sup> and subjected them to proliferation assay. Consistent with  
31 previous similar findings,<sup>9</sup> only the immortalized C5N cells were growth-inhibited by  
32 dexamethasone, in a concentration-dependent manner. P6, B9, A5 and CarB cells continued  
33 to proliferate despite dexamethasone presence (Fig. 1a). Dexamethasone induced no effect  
34 in P6, B9, A5 and CarB cells, neither proliferative nor antiproliferative. On the other hand,  
35 each tested dexamethasone concentration reduced proliferation rate of the GC-responsive  
36 C5N cells in a time-dependent manner (Fig. 1b). ANOVA utilising Dunetts' T3 post-hoc  
37 analysis demonstrated that C5N cells showed significant sensitivity to dexamethasone. In  
38 particular, at 72 hours, significant loss of survival was observed at 10<sup>-8</sup>, 10<sup>-7</sup>, and 10<sup>-6</sup>  
39 concentrations (p=0.014, p=0.002, p<0.001 respectively). On the contrary, no significant  
40 difference observed between the untreated and treated P6 cells at any dexamethasone  
41 concentration (Fig. 1b). Therefore, the cells of our system were categorized to GC-sensitive  
42 (C5N; susceptible to growth inhibition by GCs) and to GC-resistant (P6, B9, A5 and CarB; no  
43 response to GCs, neither proliferative nor antiproliferative).  
44  
45  
46  
47  
48  
49  
50  
51  
52  
53  
54  
55  
56  
57  
58  
59  
60  
61  
62  
63  
64  
65

1  
2  
3  
4  
5  
6  
7  
8  
9  
10  
11  
12  
13  
14  
15  
16  
17  
18  
19  
20  
21  
22  
23  
24  
25  
26  
27  
28  
29  
30  
31  
32  
33  
34

### ***GR expression and localization status in the multistage mouse skin carcinogenesis model***

Then, we monitored GR expression and localization in each cell line of our model. First, western blot revealed an elevation of total GR levels towards more aggressive cancer stages. Nuclear GR levels gradually increase, showing an abrupt increase during B9-to-A5 transition, whereas there is a reduction of cytoplasmic GR protein levels from B9 to A5 cells, documenting a switch of the cytoplasmic-to-nuclear ratio upon B9/A5 transition, which is independent from GC presence (Fig. 2b). This tendency of GR to translocate to the nucleus during squamous-to-spindle transition was further confirmed by immunocytochemistry, which revealed cytoplasmic GR localization in C5N, P6 and B9 cells, and mixed cytoplasmic-nuclear localization in A5 and CarB cells (Fig. 2c). The GR nucleocytoplasmic translocation at the squamous-to-spindle threshold was additionally confirmed by immunofluorescence in B9 and A5 cells, which revealed a clear cytoplasmic signal in B9 cells, but an intense nuclear staining in A5 cells (Fig. 2d). To the best of our knowledge, this mixed cytoplasmic and nuclear GR localization in aggressive stages has never been reported before. To exclude the possibility that this observation is a cell-line artefact, we confirmed it immunohistochemically *in vivo*, on sections from skin tumors induced in mice following a chemical carcinogenesis protocol. Indeed, on tumors of the same animal, papilloma stage presents mainly cytoplasmic GR localization whereas in the corresponding squamous stage GR localization is more intense and gets even more intense in the spindle stage-tumors (Fig. 2e).

35  
36  
37  
38  
39  
40  
41  
42  
43  
44  
45  
46  
47  
48  
49  
50  
51  
52  
53  
54  
55  
56  
57  
58  
59  
60  
61  
62  
63  
64  
65

### ***GR is GRE-binding competent but transactivation-incompetent in the GC-resistant cells of the mouse skin carcinogenesis model***

Then, we tested whether GC-unresponsiveness of P6, B9, A5 and CarB cells is associated with reduced DNA binding of GR to GRE-containing targets. EMSAs were performed using nuclear cell extracts of C5N, P6, B9, A5 and CarB incubated with a <sup>32</sup>P-labelled double stranded oligonucleotide that contains a GRE binding site from the human metallothionin II promoter (hMTII-GRE). The binding of GR to GREs remains ligand-dependent only in the GC-sensitive C5N cell line (Fig. 3a), in contrast to the GC-resistant P6, B9, A5 and CarB cells, in which GR has acquired the ability to bind to GREs in the absence of dexamethasone (Fig. 3b). Additionally, the pattern of GR DNA binding along the five cell lines is consistent with their nuclear GR expression profile. This evidence indicates that the ability of GR to bind to GRE-containing targets through its DNA binding domain remains intact and proportional to the nuclear GR levels (Fig. 3b). Therefore, we plausibly hypothesized that although GR binds to target GREs in a ligand-independent manner in the P6, B9, A5 and CarB cells, it might be incapable of transactivating its targets, thus providing a reason for their GC-resistance. To this end, we then tested whether unresponsiveness of GC-resistant cells to GCs might be

1 associated with inability of GRE-bound GR to transactivate crucial antiproliferative targets.  
2 We used luciferase assays to monitor the ability of endogenous GR to activate the  
3 glucocorticoid-responsive enhancer of  $\beta$ -globin in the presence of dexamethasone in all  
4 mouse cell lines (Fig. 3c). Significant luciferase activity was observed only in the GC-sensitive  
5 C5N cells upon GC treatment. In parallel, using Q-PCR, we estimated the endogenous  
6 expression of the characteristic GC-responsive antiproliferative direct GR targets p57<sup>KIP2</sup><sup>31</sup>  
7 and GILZ (Glucocorticoid-induced leucine zipper)<sup>32</sup> in dexamethasone-treated versus  
8 dexamethasone-untreated cells. In agreement with the luciferase assay findings, both targets  
9 were significantly induced in the GC-responsive C5N cells upon dexamethasone treatment,  
10 whereas the corresponding levels were not upregulated after addition of dexamethasone in  
11 all GC-resistant cells (Fig. 3d and 3e). However, sequencing analysis revealed that this  
12 impairment is not attributed to direct mutations in the domains of the GR gene that are  
13 responsible for the GR transactivation function (Supplementary Material 1).  
14  
15  
16  
17  
18  
19  
20  
21  
22

### ***N-bromotaurine induces antiproliferative effects in GC-resistant cancer cell lines***

23 Then, we checked whether BrTaur restores antiproliferative response in our model system.  
24 To this end, we treated cells with 25 $\mu$ M, 75 $\mu$ M, 125 $\mu$ M and 250 $\mu$ M BrTaur and subjected  
25 them to proliferation assays. This range is consistent with the therapeutic concentrations  
26 currently used, in the investigational clinical setting against inflammatory conditions and  
27 microbial infections.<sup>13,15</sup> BrTaur exerted a potent, dose-dependent antiproliferative effect in  
28 the GC-sensitive C5N and the GC-resistant P6, B9, A5 and CarB cells, which is evidenced  
29 from 125 $\mu$ M (Fig. 4a). The maternal substance taurine, from which BrTaur is produced upon  
30 reduction with HOBr, has been previously reported to exert anticancer properties<sup>33,34</sup>.  
31 Therefore, we treated cell lines with the concentration range of unbrominated taurine that  
32 corresponded to the tested concentration range of its brominated derivatives<sup>23</sup>. Taurine  
33 treatment did not affect mouse skin cancer cell proliferation in a significant, potent and  
34 consistent manner (Fig. 4b), implying that bromination of the taurine is the crucial factor for  
35 the consistent antiproliferative effect on cells. ANOVA utilising Dunetts' T3 post-hoc analysis  
36 demonstrated that P6 cells showed significant sensitivity at concentrations over 75 $\mu$ M  
37 bromotaurine. A5, B9 and CarB cell lines demonstrated sensitivity at concentrations over  
38 125 $\mu$ M bromotaurine. The GC-responsive C5N cells are the least sensitive to bromotaurine.  
39 The BrTaur antiproliferative effect was reproduced in GC-resistant human cancer cells of  
40 epithelial origin, i.e. the prostate cancer cell line PC3 (Fig. 4c) and the breast cancer cell line  
41 MDA-MB-231 (Fig. 4d)<sup>35,36</sup> in the tested concentration range.  
42  
43  
44  
45  
46  
47  
48  
49  
50  
51  
52  
53  
54  
55  
56  
57

### ***N-bromotaurine inhibits cell cycle progression in GC-resistant cells***

58  
59  
60  
61  
62  
63  
64  
65

1 Unlike dexamethasone (Fig. 5a), BrTaur induced antiproliferative effects on the GC-resistant,  
2 aggressive CarB cells in a concentration- and time- dependent manner (Fig. 5b). GCs inhibit  
3 cancer cell growth, at least in part, by blocking cell cycle at the G0/G1 phase. This ability of  
4 GCs to induce G1-arrest is often compromised in GC-resistant cancer cells.<sup>30</sup> In this context,  
5 we examined whether BrTaur bypasses lack of antiproliferative response in the GC-resistant  
6 cells by restoring G1-arrest. Using FACS analysis, we estimated the effect of three different  
7 BrTaur concentrations (125µM, 250µM and 500µM) on the G0/G1, S and G2/M phases, using  
8 the most aggressive GC-resistant cell line of our model system, i.e. CarB. Dexamethasone  
9 was used as the comparator substance and untreated cells were used as negative control.  
10 Dexamethasone was unable to induce G1-arrest, thus having an effect on cell cycle  
11 progression identical to the one observed for the GC-untreated cells. On the contrary, BrTaur  
12 in the concentrations of 125µM and 250µM enhanced the percentage of cells in G1 phase,  
13 thus simulating the effect of GCs on cell cycle. Interestingly, in the high, yet clinically  
14 physiological, concentration of 500µM, BrTaur potentially affected both G1 and G2 phases,  
15 demonstrating a broader ability to target cell cycle. Its effect on the S phase is moderate and  
16 seems to be dose-dependent (Fig. 5c). The experiment was performed in triplicates and  
17 presented a p value <0.05 (t-test).  
18  
19  
20  
21  
22  
23  
24  
25  
26  
27  
28  
29

30 ***Ciplatin efficacy on GC-resistant cells is potentiated by N-bromotaurine: the earlier the***  
31 ***initiation of N-bromotaurine co-administration, the more enhanced the synergistic***  
32 ***effect***  
33  
34

35 In clinical cancer therapeutics, GCs are routinely co-administered with cisplatin, either as  
36 adjuvant agents or to mitigate cisplatin adverse events. Therefore, for a substance to  
37 clinically qualify as a GC-substitute in the context of cancer, it should be able to enhance  
38 cisplatin's effects on tumor growth. To test if this applies for N-bromotaurine, we treated the  
39 GC-resistant aggressive spindle CarB cells of the mouse carcinogenesis model with a  
40 combination regimen of cisplatin plus N-bromotaurine. Three treatment schemes were used:  
41 a) pre-treatment, i.e. BrTaur 0-48h, followed by cisplatin 24-48h; b) concurrent treatment, i.e.  
42 BrTaur plus cisplatin, 0-48h; c) post-treatment, i.e. cisplatin 0-24h, followed by BrTaur 24-  
43 48h. Since the qualitative effect of BrTaur on cell cycle progression is dose-dependent for the  
44 higher 250µM (affects G1) and 500µM (affects both G1 and G2) concentrations (Fig. 5c), we  
45 tested both concentrations in the BrTaur-containing combination regimens. Each scheme was  
46 compared versus its corresponding comparator combination regimen of cisplatin plus 10<sup>-7</sup>M  
47 dexamethasone. Strikingly, both BrTaur concentrations in all-three schemes synergized  
48 efficiently with 2.9µg/mL cisplatin (a value corresponding to the cisplatin concentration  
49 efficient to kill 27% of CarB cells; CarB IC50:3.7µg/mL) (Supplementary Material 2),  
50 demonstrating significant superiority versus the corresponding comparator cisplatin plus  
51  
52  
53  
54  
55  
56  
57  
58  
59  
60  
61  
62  
63  
64  
65



1 dexamethasone regimens (Fig. 5d-f). ANOVA applying Dunnet's T3 post-hoc test showed  
2 that both BrTaur concentrations were efficient in all-three schemes ( $p \leq 0.001$ ). The most  
3 potent synergistic effect was observed for the pre-treatment scheme, where both doses of  
4 250 $\mu$ M and 500 $\mu$ M achieved similar efficacy. The synergistic effect was dose-dependent in  
5 concurrent treatment and post-treatment protocols. On the contrary, dexamethasone addition  
6 did not result to significant increase of the anti-proliferative effect of the regimen, either  
7 before, concurrently or following cisplatin treatment. Overall, the earlier the BrTaur co-  
8 administration started, the better its synergistic effect with cisplatin on CarB cell growth  
9 inhibition. Among the three treatment schemes, the inhibitory effect of cisplatin on cell growth  
10 was less potent in the post-treatment protocol; however higher doses of BrTaur were able to  
11 compensate for the delay of initiation of BrTaur co-administration (Fig 5f, fourth column).  
12  
13  
14  
15  
16  
17  
18  
19

## 20 DISCUSSION

21 Analogous to the microbes that develop a plethora of strategies to eventually become  
22 resistant to antibiotics, cancer cells invent several strategies to impair GR and overcome GC-  
23 sensitivity.<sup>2</sup> In several cases, a singleton cause of impairment cannot be identified, because  
24 GC-resistance is rather multifactorial and attributed to orchestrated inactivation of several  
25 GR-controlled pathways.<sup>2,7,8</sup> In this context, trying to identify impaired GR pathway(s)  
26 underlying GC-resistance and develop *de novo* a druggable molecule to restore  
27 responsiveness poses as a herculean task. A different approach to bypass GC-  
28 unresponsiveness of cancer cells would be to reposition alternatives from the pharmaceutical  
29 arsenal that are either approved or in late-stages of clinical trials for other GC-refractory  
30 inflammatory conditions. Given the emerging commonalities between inflammation and  
31 cancer, those alternatives might pose as latent substitutes of GCs' antiproliferative effect,  
32 awaiting in a "diamond-in-a-rough" state to be revisited in the context of cancer. This might  
33 decrease the pressure for natural selection of cancer cells that overcome the GC  
34 antiproliferative effects by deactivating their GR receptor and/or the GR-mediated pathways,  
35 the same way that prudent use of antibiotics or use of interchangeable antibiotics prevents  
36 the development of antibiotic-resistant microbe strains. Using GC-substitutes before ending-  
37 up prescribing GCs would also enable clinical oncologists to reserve the GC-based  
38 therapeutic options as a last-resort for aggressive tumors, without risking a possible induction  
39 of GC-resistance in earlier tumor stages.  
40  
41  
42  
43  
44  
45  
46  
47  
48  
49  
50  
51  
52

53 To test this hypothesis we considered the mouse skin carcinogenesis system as our  
54 basal screening tool kit. Overall, the characteristics of our study system in terms of GC-  
55 sensitivity/GC-resistance and the underlying GR status are summarized in Table II. The  
56 model includes a GC-sensitive cell line C5N which retains a functional GR and can be used  
57 as the positive, comparative screening control cell line of the panel. The rest of the cell lines  
58  
59  
60  
61  
62  
63  
64  
65

1 represent GC-resistant papillomas, squamous and spindle cells. In terms of localization, we  
2 additionally observed a GR accumulation in the nucleus during transition from squamous-to-  
3 spindle stages, resulting to a mixed cytoplasmic and nuclear signal in spindle cells. This  
4 unexpected and previously unreported finding, which was reconfirmed in *in vivo* mouse  
5 spindle skin cancer tumors, indicates the possible existence of an heterogenous population of  
6 GR isoforms and/or variants, some of which may have dominant negative function to the  
7 typical full-length isoforms. From the pathology point of view, this means that GR nuclear  
8 localization may not be a positive clinical indication for GC-responsiveness, as originally had  
9 been suggested <sup>37</sup>, especially given the fact that several dominant negative GR isoforms or  
10 splice variants that antagonize functional, full-length GR, and cause GC-unresponsiveness  
11 are also localized in the nucleus.<sup>1,2</sup>These issues will be clarified in future studies.

12 BrTaur, our first study case to be checked with our system, presents overlapping  
13 characteristics with GCs and is topically used in skin inflammatory conditions, such as acne  
14 vulgaris, instead of steroids <sup>13</sup>. It is well-tolerated and presents insignificant side-effects.<sup>13,15</sup>  
15 BrTaur surrogated for the antiproliferative effect on GC-sensitive and GC-resistant cells, thus  
16 providing the first evidence for its potential to be used interchangeably to GCs in the context  
17 of cancer, in the same concept they are currently clinically used interchangeably to GCs in  
18 the context of chronic inflammations and microbial infections. The fact that BrTaur efficiently  
19 synergizes with cisplatin to inhibit growth of GC-resistant cells further highlights its GC-  
20 mimicking therapeutic effect. The antiproliferative effect is strongly linked to the bromine  
21 moiety of the bromotaurine molecule and is mediated by inhibition of cell cycle in GC-  
22 resistant cells. The ability of BrTaur to produce a more consistent anticancer effect than  
23 taurine could be explained by the fact that the former is the oxidizing form, while the latter is  
24 the maternal, reservoir substance, considered as a pro-drug. In detail, taurine is retained in  
25 several tissues, primarily in liver, and is recruited in tissues undergoing oxidative stress by  
26 topically-produced HOCl and HOBr to finally be oxidized to its effective taurine haloamine  
27 derivatives. These scavenge the toxicity of the excess HOCl and HOBr and pick up the torch  
28 of immunologic responses at the lesion sites, preventing inflammation and exerting anti-  
29 microbial and oxidizing properties<sup>13</sup>. In this respect, the inconsistent efficacy of taurine versus  
30 N-bromotaurine on the different cell lines of the mouse carcinogenesis system may be due to  
31 fluctuated micro-concentrations of HOBr in each different cell line milieu, thus resulting to  
32 corresponding fluctuations in the concentration of the active BrTaur finally being formed.

33 It should be noted that overproliferation in our system, as in actual tumors, is  
34 associated with deregulation of several main pathways in addition to GR transactivation  
35 impairment.<sup>19</sup> These pathways, such as the ER $\alpha$  and AP-1 oncogenic pathways, crosstalk  
36 with GR since they are antagonized by its transrepression mode of action. Their progressive  
37 overactivation towards the aggressive stages in our system<sup>22,26,38</sup> implies a dysfunctional GR

1 transrepression mode additionally to the demonstrated impairment of GR transactivation  
2 mode. Furthermore, the mixed cytoplasmic and nuclear signal detected in aggressive stages  
3 of skin cancer indicates the possible existence of a heterogeneous population of GR isoforms  
4 and/or variants, some of which may have dominant negative function to the typical full-length  
5 isoforms. This could be an additional reason for GR's inability to transactivate its targets and,  
6 thus, to subsequently mediate the antiproliferative effects of GCs in GC-resistant cells. This  
7 would mean that multiple factors causing GC-resistance are possibly accumulating towards  
8 the most aggressive stages. Therefore, our system must not be seen as a model dedicated to  
9 the study of a single GC-resistance cause. Rather, it should be cautiously used as a tool kit  
10 for performing preliminary screenings in order to discriminate the alternative agents with no  
11 antiproliferative action from the ones with the potential to restore antiproliferative response in  
12 GC-resistant cells.

13  
14  
15  
16  
17  
18  
19  
20 Notably, although skin cancers are primarily associated with impairment of the GR/GC  
21 axis, they are not treated with GCs. Thus our model is not proposed as a means to spot GC-  
22 substitutes against this cancer type. However, it is the demonstrated ability of this skin  
23 cancer-based artificial model to produce results that are extrapolated to several other types of  
24 epithelial cancers<sup>21</sup>, including the ones that are commonly treated with GCs, that gives this  
25 model an added value as an emerging generalized screening tool kit for identifying GC-  
26 substitutes. Using this basal screening tool, substances that are suspected, based on medical  
27 experience in the clinic, to have overlapping profiles with GCs could be confirmed as GC-  
28 substitutes before being repurposed for the management of cancer patients. Based on this  
29 screening tool, investigational N-bromotaurine was shown to act as a GC-substitute, while its  
30 effects were reproduced in cancer types that are commonly treated with GCs, such as the  
31 GC-resistant human breast and prostate cancer cell lines. Further confirmation of this anti-  
32 tumor effect in experimental animals in future studies could accelerate subsequent  
33 repositioning of BrTaur for the management of clinical cancer patients.

34  
35  
36  
37  
38  
39  
40  
41  
42  
43 The point our approach highlights is that already-in-clinical-use compounds, able to  
44 consistently induce an antiproliferative phenotype in GC-resistant cells, even via molecular  
45 circuits which are currently as unknown to molecular biologists, as are unfamiliar to the GC-  
46 resistant cancer cells themselves, warrant to be unveiled and considered as possible GC-  
47 substitute therapeutic solutions. Analogous with what happens with newer generation  
48 antibiotics that catch the microbes unawares, the success of such compounds to startle  
49 cancer cells towards an antiproliferative direction may rely to their possible ability to act  
50 through pathways that the cancer cells have never been called to deactivate before in order  
51 to become aggressive. Such GC-substitutes may have the clinical potential to prolong  
52 disease free-survival, reduce tumor size, delay progression, mitigate side-effects and improve  
53 quality of life, in combination with well-established drugs, thus complying to the FDA's  
54  
55  
56  
57  
58  
59  
60  
61  
62  
63  
64  
65

1 established guidelines on cancer clinical trial end-points.  
2 (<http://www.fda.gov/downloads/Drugs/Guidances/ucm071590.pdf>).  
3

4 Last but not least, burning issues regarding BrTaur mechanism of action are awaiting  
5 to be thoroughly addressed in future studies. Potential ways for its systemic administration in  
6 the context of cancer therapeutics should also be explored. Anti-inflammatory effects of  
7 BrTaur are mediated by modification of the IkappaBalpha, an NF-kappaB inhibitor<sup>39</sup>. This  
8 interaction could also underlie BrTaur antiproliferative effects on GC-resistant cells, given that  
9 NF-kappaB stands in the cross-roads between inflammation and cancer<sup>40</sup> and is a crucial  
10 effector of GR-mediated tumor-suppressor effects<sup>2</sup>. Given the commonalities shared between  
11 anti-inflammatory and anti-cancer pathways, BrTaur may, at least in part, exert its anti-cancer  
12 action, in addition to its well-known anti-inflammatory properties<sup>13</sup> by targeting common  
13 networks underlying both pathological entities<sup>17,18</sup>. Comprehensive, high-throughput analyses  
14 of the molecular and cellular changes and the transcriptional programs alterations triggered  
15 upon BrTaur treatment using state-of-the-art, multiomics approaches are anticipated to shed  
16 more light on this issue in the future. The full range of BrTaur functions might extend beyond  
17 interfering with GR-mediated pathways, and is currently under investigation. The role of  
18 BrTaur in cancer emerges as a subject of fruitful research and poses as a mysterious “black  
19 box”, the decoding of which might pave the way for next generation therapeutics.  
20  
21  
22  
23  
24  
25  
26  
27  
28  
29  
30

### 31 **ACKNOWLEDGEMENTS**

32 All authors have read the journal's authorship agreement and the manuscript has been  
33 reviewed and approved by all named authors. All authors have read the journal's policy on  
34 conflicts of interest and declare that there are no conflicts of interest. SL was supported by  
35 “IKY fellowships of excellence for postgraduate studies in Greece-Siemens program” given in  
36 terms of the settlement between the Greek Government and Siemens company. ES was  
37 funded by the “Scholarships Programs by the State Scholarships Foundation” in the  
38 framework of the Operational Program "Education and Life Long Learning" within the National  
39 Strategic Reference Framework. N-bromotaurine formulation was a donation of NASCO AD.  
40 Biotechnology Laboratory, for use in this preclinical research.  
41  
42  
43  
44  
45  
46  
47  
48  
49  
50  
51  
52  
53  
54  
55  
56  
57  
58  
59  
60  
61  
62  
63  
64  
65

## REFERENCES

1. Herr I, et al. Glucocorticoid cotreatment induces apoptosis resistance toward cancer therapy in carcinomas. *Cancer Res* 2003;63:3112-20.
2. Ramamoorthy S, Cidlowski JA. Exploring the molecular mechanisms of glucocorticoid receptor action from sensitivity to resistance. *Endocr Dev* 2013;24:41-56.
3. Budunova IV, et al. Glucocorticoid receptor functions as a potent suppressor of mouse skin carcinogenesis. *Oncogene* 2003;22:3279-87.
4. Chebotaev D, Yemelyanov A, Budunova I. The mechanisms of tumor suppressor effect of glucocorticoid receptor in skin. *Mol Carcinog* 2007;46:732-40.
5. Latorre V, et al. Selective ablation of glucocorticoid receptor in mouse keratinocytes increases susceptibility to skin tumorigenesis. *J Invest Dermatol* 2013;133:2771-9.
6. Herr I, Pfitzenmaier J. Glucocorticoid use in prostate cancer and other solid tumours: implications for effectiveness of cytotoxic treatment and metastases. *Lancet Oncol* 2006;7:425-30.
7. Lambrou GI, et al. Glucocorticoid and proteasome inhibitor impact on the leukemic lymphoblast: multiple, diverse signals converging on a few key downstream regulators. *Mol Cell Endocrinol* 2012;351:142-51.
8. Copland JA, et al. Sex steroid receptors in skeletal differentiation and epithelial neoplasia: is tissue-specific intervention possible? *Bioessays* 2009;31:629-41.
9. Spiegelman VS, et al. Resistance of transformed mouse keratinocytes to growth inhibition by glucocorticoids. *Mol Carcinog* 1997;20:99-107.
10. Piovan E, et al. Direct reversal of glucocorticoid resistance by AKT inhibition in acute lymphoblastic leukemia. *Cancer Cell* 2013;24:766-76.
11. Allison M. NCATS launches drug repurposing program. *Nat Biotechnol* 2012;30:571-2.
12. Barnes PJ, Adcock IM. Glucocorticoid resistance in inflammatory diseases. *Lancet* 2009;373:1905-17.
13. Marcinkiewicz J, Kontny E. Taurine and inflammatory diseases. *Amino Acids* 2014;46:7-20.
14. Islambulchilar M, et al. Taurine attenuates chemotherapy-induced nausea and vomiting in acute lymphoblastic leukemia. *Amino Acids* 2015;47:101-9.
15. Marcinkiewicz J, et al. Topical taurine bromamine, a new candidate in the treatment of moderate inflammatory acne vulgaris: a pilot study. *Eur J Dermatol* 2008;18:433-9.
16. Gottardi W, Nagl M. N-chlorotaurine, a natural antiseptic with outstanding tolerability. *J Antimicrob Chemother* 2010;65:399-409.
17. Wogan GN, et al. Infection, inflammation and colon carcinogenesis. *Oncotarget* 2012;3:737-8.
18. Rayburn ER, Ezell SJ, Zhang R. Anti-Inflammatory Agents for Cancer Therapy. *Mol Cell Pharmacol* 2009;1:29-43.
19. Zoumpourlis V, et al. Alterations in signal transduction pathways implicated in tumour progression during multistage mouse skin carcinogenesis. *Carcinogenesis* 2003;24:1159-65.
20. Skourtis E, et al. Progression of mouse skin carcinogenesis is associated with the orchestrated deregulation of miR-200 family members, miR-205 and their common targets. *Mol Carcinog* 2015.
21. Balmain A, Yuspa SH. Milestones in skin carcinogenesis: the biology of multistage carcinogenesis. *J Invest Dermatol* 2014;134:E2-7.
22. Logotheti S, et al. Progression of mouse skin carcinogenesis is associated with increased ERalpha levels and is repressed by a dominant negative form of ERalpha. *PLoS One* 2012;7:e41957.
23. Olszanecki R, et al. The role of heme oxygenase-1 in down regulation of PGE2 production by taurine chloramine and taurine bromamine in J774.2 macrophages. *Amino Acids* 2008;35:359-64.

24. Daskalos A, et al. Global DNA hypomethylation-induced DeltaNp73 transcriptional activation in non-small cell lung cancer. *Cancer Lett* 2011;300:79-86.
25. Karakaidos P, et al. Overexpression of the replication licensing regulators hCdt1 and hCdc6 characterizes a subset of non-small-cell lung carcinomas: synergistic effect with mutant p53 on tumor growth and chromosomal instability--evidence of E2F-1 transcriptional control over hCdt1. *Am J Pathol* 2004;165:1351-65.
26. Papassava P, et al. Overexpression of activating transcription factor-2 is required for tumor growth and progression in mouse skin tumors. *Cancer Res* 2004;64:8573-84.
27. Solakidi S, Psarra AM, Sekeris CE. Differential distribution of glucocorticoid and estrogen receptor isoforms: localization of GRbeta and ERalpha in nucleoli and GRalpha and ERbeta in the mitochondria of human osteosarcoma SaOS-2 and hepatocarcinoma HepG2 cell lines. *J Musculoskelet Neuronal Interact* 2007;7:240-5.
28. Logotheti S, et al. Sp1 binds to the external promoter of the p73 gene and induces the expression of TAp73gamma in lung cancer. *FEBS J* 2010;277:3014-27.
29. Vlahopoulos S, et al. Recruitment of the androgen receptor via serum response factor facilitates expression of a myogenic gene. *J Biol Chem* 2005;280:7786-92.
30. Mattern J, Buchler MW, Herr I. Cell cycle arrest by glucocorticoids may protect normal tissue and solid tumors from cancer therapy. *Cancer Biol Ther* 2007;6:1345-54.
31. Samuelsson MK, et al. p57Kip2, a glucocorticoid-induced inhibitor of cell cycle progression in HeLa cells. *Mol Endocrinol* 1999;13:1811-22.
32. Ayroldi E, Riccardi C. Glucocorticoid-induced leucine zipper (GILZ): a new important mediator of glucocorticoid action. *FASEB J* 2009;23:3649-58.
33. Kim T, Kim AK. Taurine enhances anticancer activity of cisplatin in human cervical cancer cells. *Adv Exp Med Biol* 2013;776:189-98.
34. Zhang X, et al. Taurine induces the apoptosis of breast cancer cells by regulating apoptosis-related proteins of mitochondria. *Int J Mol Med* 2015;35:218-26.
35. Martin-Sabroso C, et al. Overcoming glucocorticoid resistances and improving antitumor therapies: lipid and polymers carriers. *Pharm Res* 2015;32:968-85.
36. Karmakar S, Jin Y, Nagaich AK. Interaction of glucocorticoid receptor (GR) with estrogen receptor (ER) alpha and activator protein 1 (AP1) in dexamethasone-mediated interference of ERalpha activity. *J Biol Chem* 2013;288:24020-34.
37. Antakly T, Thompson EB, O'Donnell D. Demonstration of the intracellular localization and up-regulation of glucocorticoid receptor by in situ hybridization and immunocytochemistry. *Cancer Res* 1989;49:2230s-2234s.
38. Zoumpourlis V, et al. High levels of phosphorylated c-Jun, Fra-1, Fra-2 and ATF-2 proteins correlate with malignant phenotypes in the multistage mouse skin carcinogenesis model. *Oncogene* 2000;19:4011-21.
39. Tokunaga S, Kanayama A, Miyamoto Y. Modification of IkappaBalpha by taurine bromamine inhibits tumor necrosis factor alpha-induced NF-kappaB activation. *Inflamm Res* 2007;56:479-86.
40. Karin M. NF-kappaB as a critical link between inflammation and cancer. *Cold Spring Harb Perspect Biol* 2009;1:a000141.

## FIGURE LEGENDS

1  
2  
3  
4  
5  
6  
7  
8  
9  
10  
11  
12  
13  
14  
15  
16  
17  
18  
19  
20  
21  
22  
23  
24  
25  
26  
27  
28  
29  
30  
31  
32  
33  
34  
35  
36  
37  
38  
39  
40  
41  
42  
43  
44  
45  
46  
47  
48  
49

**Figure 1:** Estimation of responsiveness of cell lines of the mouse skin carcinogenesis model to GCs (dexamethasone) by crystal violet assays. **(a)** In the representative time point of 48h, the number of cells drastically decreases proportional to dexamethasone concentration in comparison with the untreated cells in the C5N cell line (expressed as ratio to untreated cells). In contrast, there is no change in cell numbers of dexamethasone-treated P6, B9, A5 and CarB cells compared to their corresponding untreated controls, in any of the concentrations tested. **(b)** The profile of the antiproliferative action of GCs on the GC-sensitive C5N cells over time, for each of the tested dexamethasone concentrations in comparison to a selected GC-resistant cell line P6. The experiments were performed in triplicates.

50  
51  
52  
53  
54  
55  
56  
57  
58  
59  
60  
61  
62  
63  
64  
65

**Figure 2:** GR is translocated in nucleus during transition from squamous to spindle stage of skin carcinogenesis. **(a)** GR protein expression levels of total (tGR), cytoplasmic (cGR) and nuclear (nGR) extracts of the mouse skin carcinogenesis model. **(b)** Western blot results indicate a switch in the cytoplasmic-to-nuclear GR ratio (cGR-to-nGR) during transition from squamous to spindle stage. **(c)** Immunocytochemistry analysis of the panel of mouse skin carcinogenesis model with anti-GR antibody revealed cytoplasmic staining in C5N, P6 and B9 cells, and mixed cytoplasmic and nuclear staining in A5 and CarB cells. The black arrows indicate GR-stained nuclei. These immunocytochemical patterns were rather uniform in the above mentioned cell lines. **(d)** The immunofluorescence GR signal is cytoplasmic in the squamous B9 cells, but nuclear in the spindle A5 cells. **(e)** Immunohistochemistry using anti-GR antibody in paraffin-embedded tissues isolated from the papilloma, squamous and spindle stage of the same chemically-induced tumor in one mouse revealed higher number of GR-stained nuclei in spindle cells in comparison with the corresponding papilloma and squamous stage. Each figure represents a 200x magnitude, whereas the upper-right boxes in each figure represent a 400x magnitude. The black boxes represent the magnified area. The black arrows indicate GR-stained nuclei.

**Figure 3:** GR is DNA binding-competent but transactivation-incompetent in GC-resistant cell lines of the mouse skin carcinogenesis model. **(a)** Electrophoretic mobility shift assay in the GC-responsive C5N revealed binding activity of GR to glucocorticoid responsive elements (GRE) only upon dexamethasone (C5N+dex) treatment. **(b)** EMSA assay for GR using nuclear extracts demonstrated binding activity of GR to glucocorticoid responsive elements (GRE) of the GC-unresponsive P6, B9, A5 and CarB cells in the absence of dexamethasone signal. DNA binding increases directly proportional to the demonstrated nuclear GR protein

1 levels towards more aggressive cell lines. Specificity of the EMSA reaction is confirmed by  
2 supershift reactions in A5 (lane 6) cells using anti-GR antibody. **(c)** Luciferase assays in the  
3 GC-sensitive and the GC-resistant cells of the mouse skin carcinogenesis model co-  
4 transfected with the 17m-GRE-G-Luc, in dexamethasone absence (-dex) or presence (+dex).  
5 Luciferase expression is significantly induced (One asterisk (\*) denotes  $p < 0.05$ ) only in the  
6 GC-sensitive C5N cells upon dexamethasone treatment. Error bars represent the standard  
7 error of the mean. Two-tailed p values are derived from independent t-tests. Three  
8 biological replicates were available for each experiment. **(d)** Box plots demonstrating the  
9 transcription induction of GILZ under dexamethasone treatment in the GC-sensitive and  
10 the GC-resistant cell lines before (-dex) and after (+dex) dexamethasone treatment,  
11 estimated by qPCR. The relative quantification (RQ) values in  $\log_{10}$  are shown. For each cell  
12 line, the untreated control was used as calibrator. The housekeeping gene beta-2  
13 microglobulin was used as an internal control of mRNA Q-PCR expression. The experiments  
14 were performed in triplicates. **(e)** Same as 3d, for p57<sup>KIP2</sup> mRNA levels. In both genes,  
15 significant induction is only observed in C5N cells (indicated by star). RQ: relative  
16 quantification value.  
17  
18  
19  
20  
21  
22  
23  
24  
25  
26  
27  
28  
29

30 **Figure 4:** Estimation of the antiproliferative response of the GC-sensitive and the GC-  
31 resistant cell lines to N-bromotaurine by proliferation assays. **(a)** In the representative time  
32 point of 48h, the number of cells drastically decreases in comparison with the corresponding  
33 untreated control cells for all cell lines of the study model (expressed as ratio to untreated  
34 cells). **(b)** Comparative treatment of the cells with the maternal substance taurine did not  
35 affect mouse skin cancer cell proliferation in a significant and consistent manner, implying  
36 that bromination of the taurine is the crucial factor for the consistent antiproliferative effect on  
37 cells. **(c)** The profile of the antiproliferative action of N-bromotaurine on the GC-resistant GC-  
38 resistant prostate cancer PC3. **(d)** Same as 4c for the human GC-resistant prostate cancer  
39 MDA-MB-231. The experiments were performed in triplicates.  
40  
41  
42  
43  
44  
45  
46  
47

48 **Figure 5:** Comparison of the antiproliferative response of the aggressive GC-resistant cells to  
49 GCs versus N-bromotaurine. **(a)** proliferation assays on CarB cells treated with  
50 dexamethasone reveal lack of significant antiproliferative response of CarB upon addition of  
51 GCs over time, as evidenced by the OD measurements. **(b)** In contrast, proliferation assays  
52 on CarB cells treated with N-bromotaurine instead of dexamethasone reveal restoration of  
53 antiproliferative response of CarB cells by N-bromotaurine over time. The restoration of  
54 antiproliferative response is statistically significant in the 250 $\mu$ M concentration, after 48 and  
55 72 hours of N-bromotaurine treatment. Three independent experiments were performed, each  
56  
57  
58  
59  
60  
61  
62  
63  
64  
65



1  
2  
3  
4  
5  
6  
7  
8  
9  
10  
11  
12  
13  
14  
15  
16  
17  
18  
19  
20  
21  
22  
23  
24  
25  
26  
27  
28  
29  
30  
31  
32  
33  
34  
35  
36  
37  
38  
39  
40  
41  
42  
43  
44  
45  
46  
47  
48  
49  
50  
51  
52  
53  
54  
55  
56  
57  
58  
59  
60  
61  
62  
63  
64  
65

in triplicate. The means+SEM values are shown in the graphs. **(c)** FACS analysis of N-bromotaurine-treated CarB cells (CarB + BrTaur) compared with dexamethasone-treated CarB cells (CarB + dex) and untreated CarB cells (CarB). BrTaur, at concentrations of 125µM and 250µM, increased the number of cells in G0/G1 phase; whereas at the high concentration of 500µM, BrTaur drastically decreased both G0/G1 and G2/M phases. Dexamethasone, at 10<sup>-7</sup>M concentration failed to significantly affect the number of cells in G1/G0 phase. Corresponding summary graphs for each phase of the cell cycle (means±SEM from 3 independent FACS analyses measurements) derived by comparison of untreated CarB cells each of the dexamethasone-treated, 125µM BrTaur-treated, 250µM BrTaur-treated and 500µM BrTaur-treated CarB cells. **(d-f)** 250µM BrTaur-treated and 500µM BrTaur-treated CarB cells synergized efficiently with 2.9 cisplatin (cis) after 48hours of BrTaur plus cisplatin combination therapy as **(d)** pre-treatment (BrTaur + cis), **(e)** concurrent treatment (cis/BrTaur) or **(f)** post-treatment (cis + BrTaur). Results are flagged with no asterisk when p-value is more than 0.05, and with two asterisks when the p-value is less than 0.001.(See text for details on treatment schemes of 5d-f).

**Table I:** Primers used for Q-PCR reactions

Q-PCR amplicon	Primers	Primer sequence	Annealing temperature
p57 <sup>KIP2</sup>	F	5- CCTCTTCGGGCCTGTAGAC -3	59°C
	R	5- CACCGTCTCGCGGTAGAA -3	
GILZ	F	5-TAACACTGTCTGGTAACGATGTAA-3	
	R	5-TAACACTGTCTGGTAACGATGTAA-3	
β2-microglobulin	F	5- GCATGGCTCGCTCGGTGAC -3	
	R	5- GCGTATGTATCAGTCTCAGTG-3	

**Table II:** Mouse skin carcinogenesis model features, in correlation with aspects of GR status in each cell line of the model.

Model features GR features	INITIATION	PROMOTION		PROGRESSION	
	C5N	P6	B9	A5	CarB
	GC-sensitive	GC-resistant	GC-resistant	GC-resistant	GC-resistant
<b>EXPRESSION</b>					
Nuclear GR levels	+	+	++	++++	++++
<b>LOCALIZATION</b>					
GR localization	cyt	cyt	cyt	nucl+cyt	nucl+cyt
<b>DNA BINDING</b>					
binding to GRE elements	+	+	++	++++	++++
<b>TRANSACTIVATION MODE</b>					
Transactivation of GC-responsive antiproliferative GRE-containing targets	+	-	-	-	-
Mutation in GR transactivation domains (exons 2, 5 and 9)	NO	NO	NO	NO	NO
<b>TRANSREPRESSION MODE</b>					
Active AP-1 pathway <sup>38</sup>	+	++	+++	++++	++++
Active ER $\alpha$ pathway <sup>22</sup>	+	++	++++	++++	++++

cyt: cytoplasmic; nucl: nuclear

The bold line of the table represents the threshold between promotion and progression stages in the mouse skin carcinogenesis system.

Figure 1  
[Click here to download high resolution image](#)

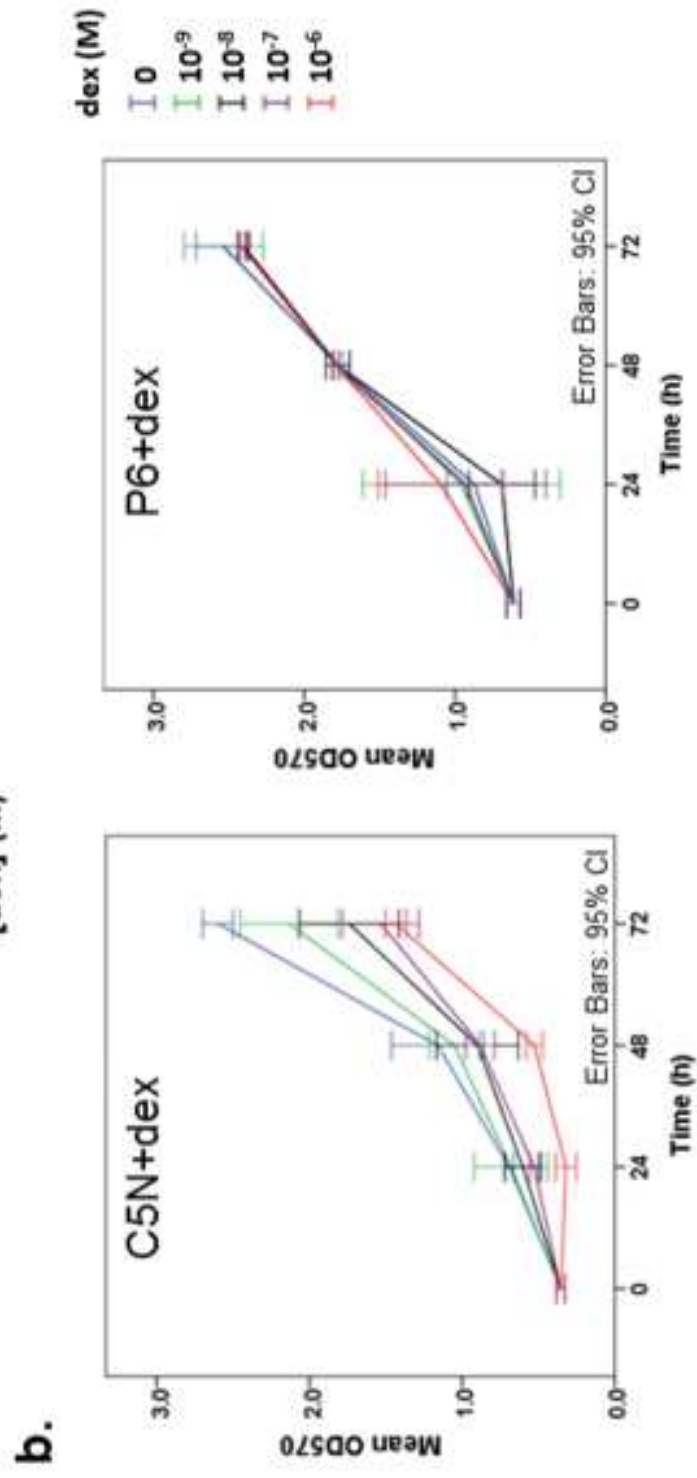
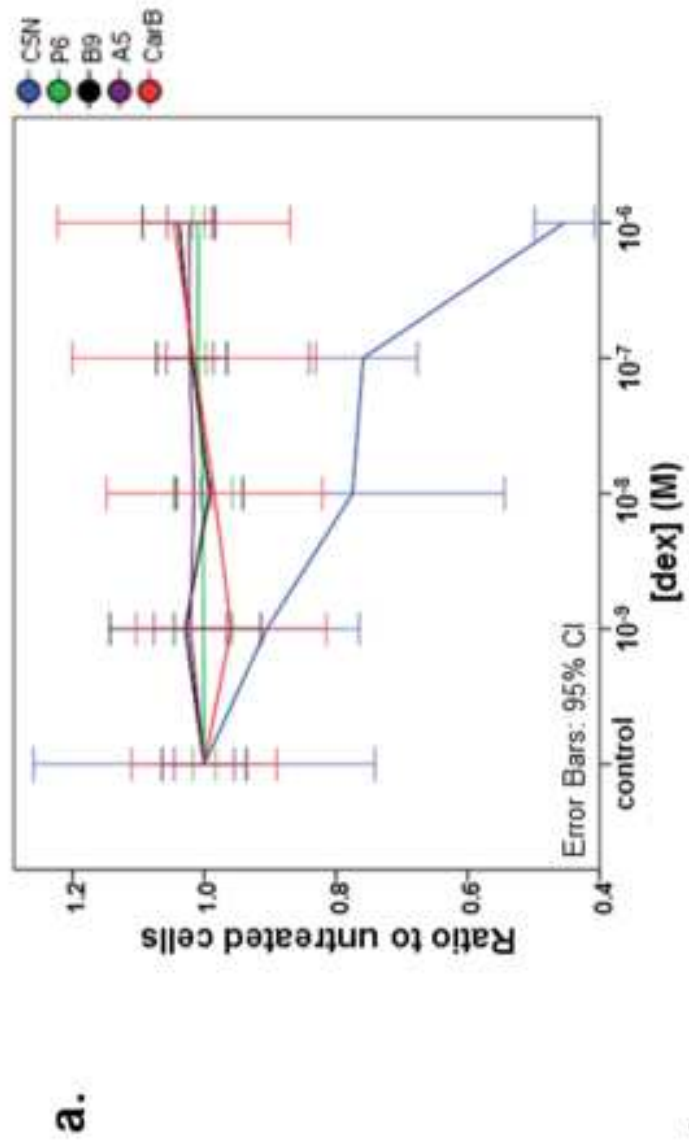
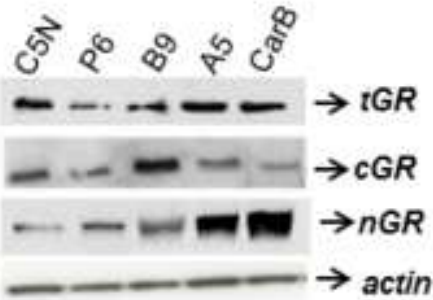
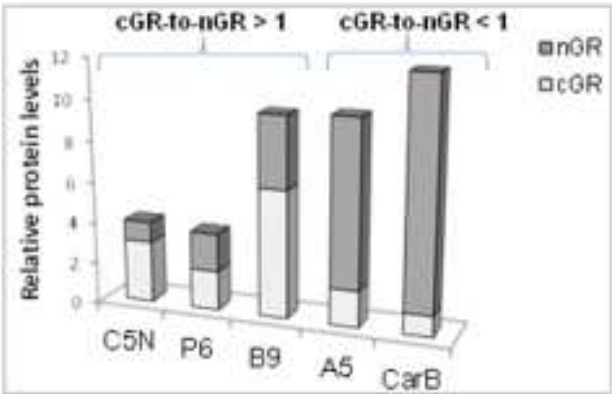


Figure 2  
[Click here to download high resolution image](#)

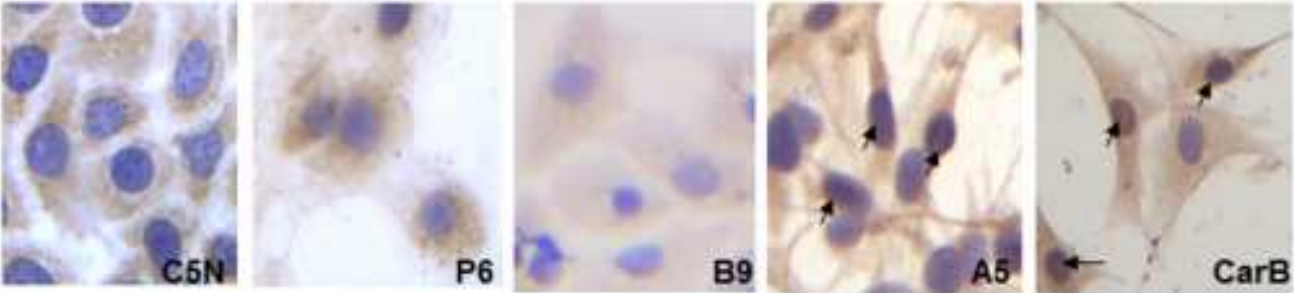
a.



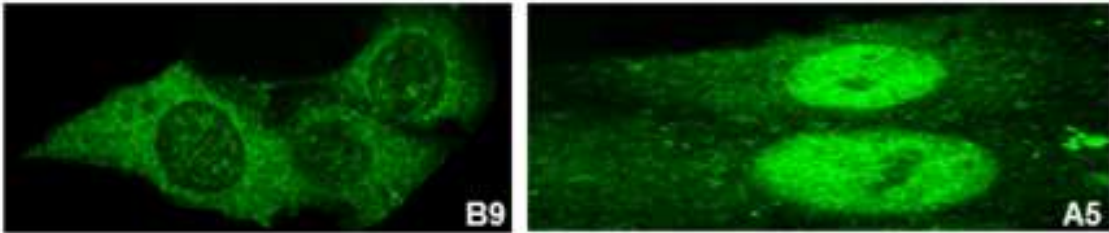
b.



c.



d.



e.

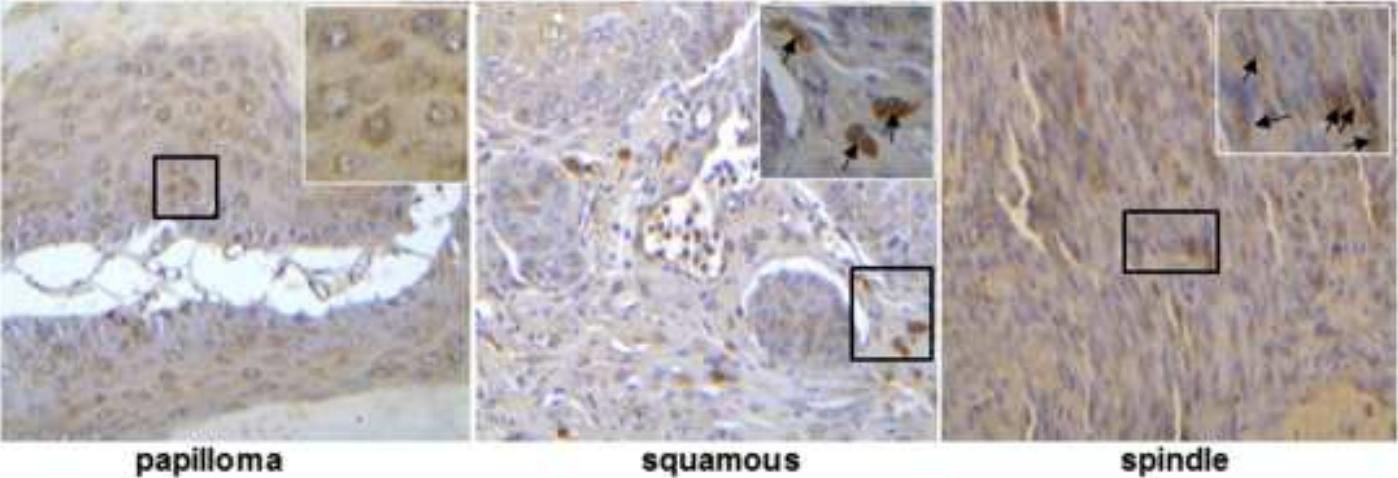


Figure 3  
[Click here to download high resolution image](#)

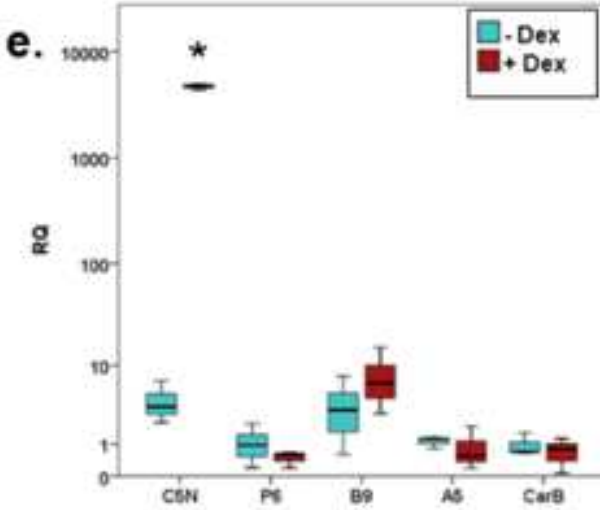
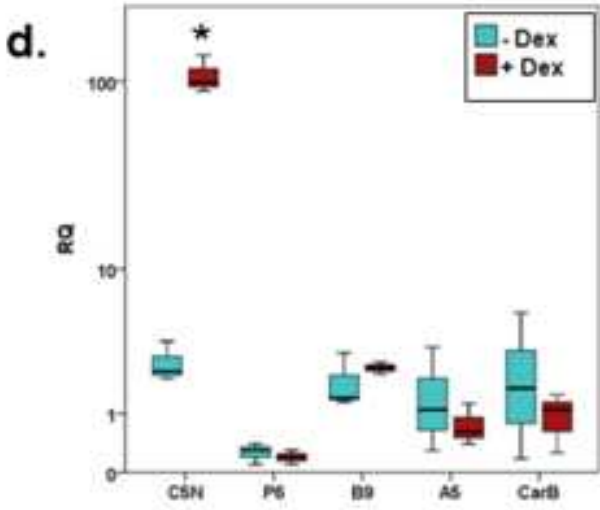
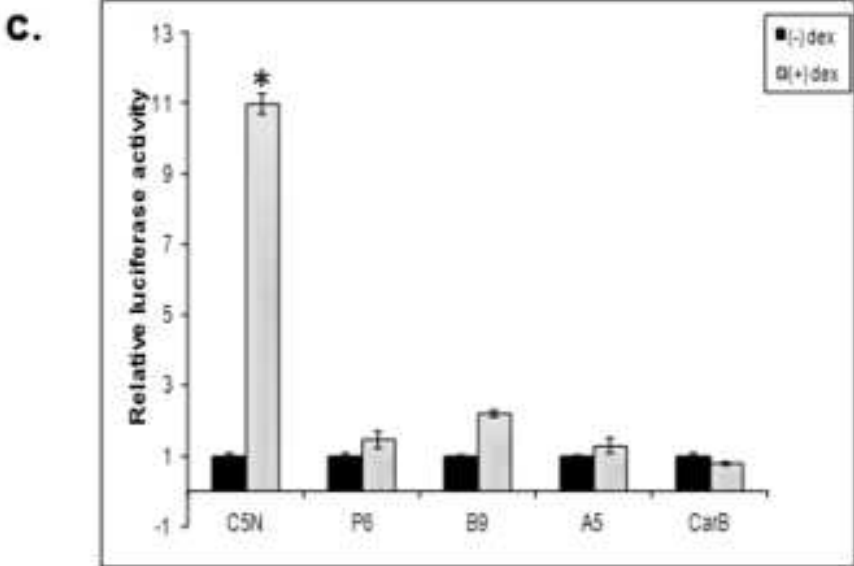
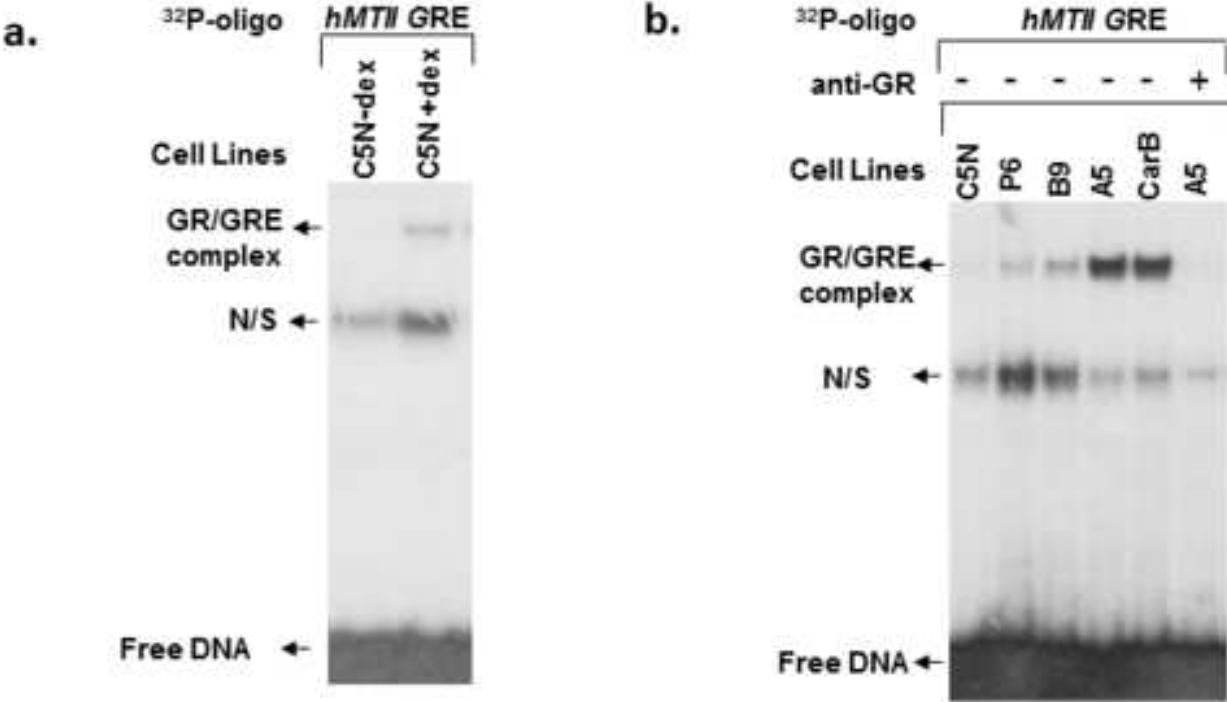


Figure 4  
[Click here to download high resolution image](#)

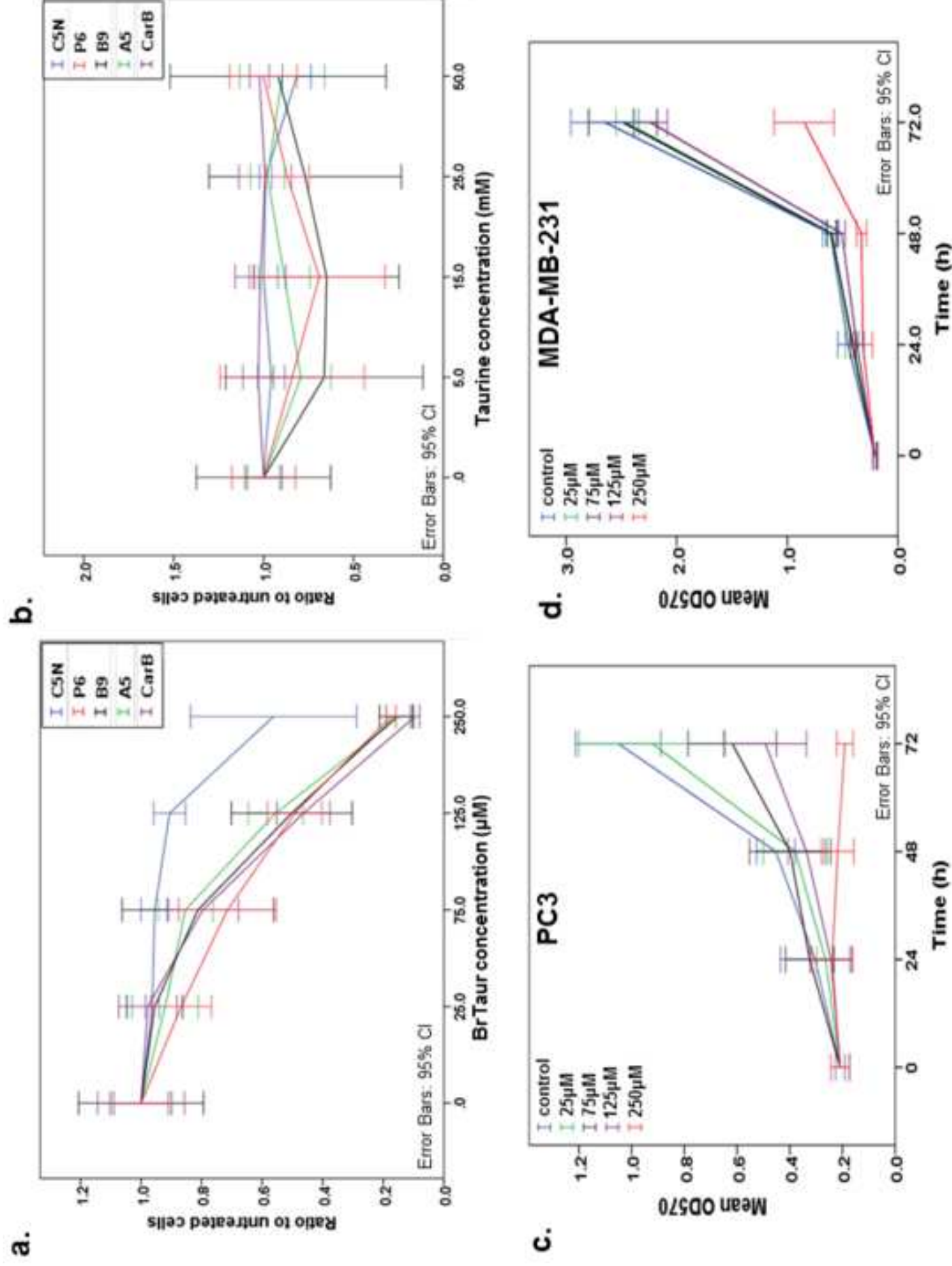
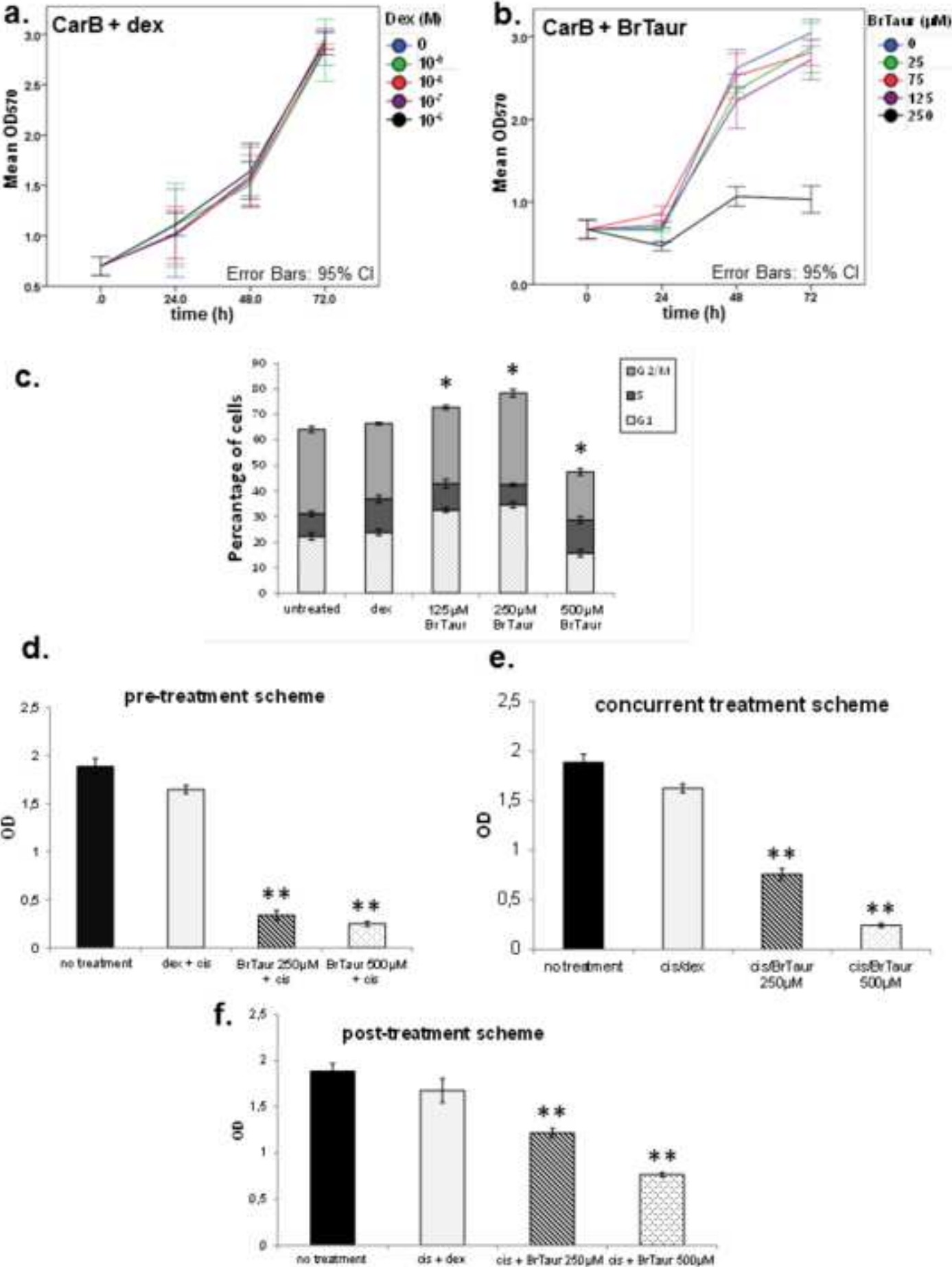


Figure 5  
[Click here to download high resolution image](#)





**Supplementary material 1**

[Click here to download Supplemental Tables/Figures: Supplementary material.docx](#)

**Supplementary material 2**

[Click here to download Supplemental Tables/Figures: Supplementary material 2.pptx](#)